Deubiquitinase USP8 targets ESCRT-III to promote incomplete cell division

Juliette Mathieu, Pascale Michel-Hissier, Virginie Boucherit, Jean-René Huynh

Deubiquitinase USP8 targets ESCRT-III to promote incomplete cell division

Juliette Mathieu[1*], Pascale Michel-Hissier[1] , Virginie Boucherit[1] and Jean-René Huynh[1*]

1: Collège de France, PSL Research University, CNRS, Inserm, Center for Interdisciplinary Research in Biology, Paris, France

*Corresponding authors: juliette.mathieu@college-de-france.fr and jean-rene.huynh@college-de-france.fr

Keywords: UBPY, abscission, cytokinesis, germline cyst, CHMP2B, CHMP4, Shrub, DUB, oogenesis, *Drosophila*

In many vertebrate and invertebrate organisms, gametes develop within groups of interconnected cells called germline cysts. Cysts form by several rounds of incomplete divisions, whose underlying molecular mechanisms remain unknown. Here, we found that loss of a single gene, encoding the deubiquitinase USP8, can transform incomplete divisions of germline cells into complete divisions. Conversely, overexpression of USP8 in germline stem cells (GSCs) is sufficient for the reverse transformation from complete to incomplete cytokinesis. We further demonstrate that CHMP2B and Shrub/CHMP4, two ESCRT-III proteins, are targets of the deubiquitinating activity of USP8. In *Usp8* mutant sister cells, ectopic recruitment of ESCRT proteins at intercellular bridges causes cysts to break apart and reducing CHMP2B or Shrub/CHMP4 levels is sufficient to suppress these abscissions. Finally, we show that a Shrub/CHMP4 variant that cannot be ubiquitinated, does not localize at abscission bridges and cannot substitute for endogenous Shrub during complete abscission of the GSCs. Taken together, our results uncover ubiquitination of ESCRT-III as a major switch between two types of cell division.

Clonal multicellularity arises by incomplete divisions of single-cell precursors and gives rise to groups of sister cells linked by cytoplasmic bridges. Such mechanisms underlie the formation of colonies of unicellular organisms and the emergence of multicellularity (*1*, *2*). It is also a conserved feature of germline cells development, which form cysts of sister cells sharing the same cytoplasm (*3*, *4*). *Drosophila* oogenesis is an attractive model system to study how cells can switch from complete to incomplete cytokinesis. Indeed, GSCs divide first completely to produce a single-cell precursor called a cystoblast (CB). Then, each CB goes through four rounds of incomplete divisions to generate germline cysts made of 16 sister cells, all linked by cytoplasmic bridges called ring canals (RC) (*5*) (Fig 1A-B). To identify new genes involved in cyst formation, we expressed a collection of sh-RNAs in the germline of *Drosophila* females, and screened for egg chambers with an abnormal number of nuclei. Two independent sh-RNA lines targeting the deubiquitinating enzyme USP8 (*6*) induced the formation of egg chambers made of 8 nuclei or less, instead of 16 (Fig 1C-E, and S1A-B). By analyzing the formation of these smaller egg chambers at earlier stages, we found that they resulted from partial breakings of cysts due to ectopic cytokinetic abscission in the germarium. Indeed, the fusome, an ER-derived organelle specific to early germ cells, formed a midbody-like structure, a feature of complete abscission, which is never seen in wild type cysts (Fig 1D, F-G and S1B-C) (*7*, *8*). We demonstrated that they were complete abscissions by showing that photoactivatable molecules were not able to diffuse from one sister cell to the next, when the midbody structure was present (Fig S1D-E, Movie 1-4). Furthermore, we observed by live-imaging the physical separation of the fusome in mutant cysts (Fig S1F-G, Movies 5 and 6). We observed similar ectopic abscissions in male germ cells upon depletion of *Usp8* (Fig S1H-I). Homozygous mutant cysts for a null allele of *Usp8* (*9*) ($Usp8^{KO}$ germ line clone, GLC) exhibited the same ectopic abscission phenotype, arguing for the specificity of these sh-RNAs (Fig 1H-I, 2C, Fig S1J-K). To rule out the possibility that complete abscissions of *Usp8*-depleted cysts were caused by de-

differentiation of cysts into GSCs (*10, 11*), we verified that *Usp8*-depleted cysts still expressed the differentiation marker Bam (Fig 1H-I). *Usp8^{KO}* GLC also lacked Nanos expression at 4-cell cysts (*12*), similarly to control differentiating cysts (Fig S1L). In addition, we found that mutant cysts could enter meiois (Fig 1M-N), and we did not detect an increase in cell death (20% (n=44) in wild type and 11% (n=27) in *sh-Usp8* cysts). Altogether, these observations indicated that *Usp8* is necessary to maintain incomplete cytokinesis in *Drosophila* germline cysts.

Conversely, we tested whether USP8 could be sufficient to inhibit cytokinesis in cells normally completing abscission such as GSCs. We overexpressed a wild type form of USP8 in these stem cells and observed the formation of stabilized cytoplasmic bridges in stem cells (aka stem-cysts (*13*), Fig 1J,K,L), which led to CBs made of two cells. These 2-cell CBs then went through 4 rounds of mitosis generating egg chambers made of 32 cells instead of 16 (Fig 1J) (*8, 13-15*). Incomplete cytokinesis in GSCs overexpressing USP8 was not caused by premature differentiation of GSCs as they did not express the cyst-specific protein Bam (Fig 1K,K'). Similarly, we found that overexpressing USP8 in somatic follicle cells surrounding germline cells and in S2 cells also led to the formation of ectopic cysts (Fig S1O-U). Taken together these results demonstrated that USP8 is necessary and sufficient to promote incomplete divisions in germline and somatic cells.

Next, we tested whether USP8 deubiquitinase activity (DUB) was required for the regulation of abscission. We expressed a catalytically inactive form of USP8, USP8-C572A (*9, 16, 17*) in *Usp8^{KO}* cysts, and found that it was unable to rescue germline cysts breaking, in contrast to wild type USP8 (Fig 2A-E, S2A-B). Similarly, overexpression of USP8-C572A was not sufficient to arrest cytokinesis nor to induce the formation of stem-cysts in GSCs, follicle cells and S2 cells (Fig 1L-M; Fig S1P, S1U). We concluded that USP8 DUB activity is required for the regulation of abscission.

To identify potential targets of this activity, we stained *Usp8* mutant cells for Ubiquitin and searched for sub-cellular regions with increased levels of ubiquitinated proteins. Besides the appearance of cytoplasmic aggregates, as described in mammals (*18*) (Fig S2C-H), we noticed an accumulation of ubiquitinated proteins at ectopic midbodies (Fig 2F-G). In addition, we found that USP8 tagged with a GFP at the endogenous locus localized at sites of cytokinesis in both males and females, i.e. midbodies of GSC/CB pairs, RCs of germline cysts and follicle cell RCs (Fig 2H-I, S2A,I-J). Altogether these data suggested that the relevant targets of USP8 could be localized at abscission sites.

The N-terminal MIT domain (contained within Microtubule-Interacting and Trafficking proteins) of human USP8 was shown to interact with ESCRT-III proteins (*19*). ESCRT-III are small proteins, which polymerize into helical filaments thought to be the driving force of several membrane scission events including abscission (*20-24*). This prompted us to investigate whether they could be targets of USP8 (*25-27*). We found that three *Drosophila* ESCRT-III proteins, CHMP1, CHMP2B and Shrub, the unique *Drosophila* homolog of CHMP4 could immunoprecipitate USP8 (Fig 3A, S3A). We also showed that

all three proteins were ubiquitinated in *Drosophila* cells (Fig 3B). Interestingly, expressing a wild type form of USP8 was sufficient to greatly reduce the amount of ubiquitinated CHMP2B and Shrub, but not of CHMP1 (Fig 3B, S3B). In contrast, the inactive USP8-C572A had no effect on the ubiquitination levels, although it could still bind all three ESCRT-III proteins (Fig 3A,B and Fig S3A,B). Conversely, knocking down *Usp8* in S2 cells led to increased levels of ubiquitinated Shrub and CHMP2B (Fig S3C,D,E). We concluded that USP8 is necessary and sufficient to deubiquitinate CHMP2B and Shrub.

We then investigated whether CHMP2B and Shrub could be relevant targets *in vivo* by first analyzing their localization in germline cells. Shrub localized at the RC and midbody of GSC/CB pairs (*8*), but, remarkably was absent at cysts RCs (Fig 3C,D and Fig S3F). A similar pattern was observed for CHMP2B (Fig S3H-I), and CHMP1 (Fig S3K-L). However, in cysts lacking *Usp8*, Shrub, CHMP2B and CHMP1 all localized at ectopic midbodies and cysts RCs (Fig 3E, S3G,J,M). Similarly, in male germ cells lacking *Usp8*, Shrub and CHMP2B localized at sites of ectopic abscission (Fig S3N-Q). To test if the ectopic localization of ESCRT-III was responsible for ectopic abscissions seen in the absence of USP8, we reduced Shrub or CHMP2B levels in *Usp8*-depleted cysts. Firstly, we removed one copy of *Shrub* in germ cells lacking USP8. In this context, we counted fewer 4-cell cysts in the process of breaking apart than in cysts depleted of USP8 alone (Fig 3F-H). In addition, we found that older egg chambers contained higher numbers of nuclei compared to *sh-Usp8* mutant egg chambers (Fig S3R). We also observed complete rescue with egg chambers made of 16 cells and a posterior oocyte, never seen in *sh-Usp8* alone (Fig 3I, J). Secondly, a reduction in CHMP2B levels in *Usp8* depleted germline was also able to rescue ectopic abscissions of mutant cysts (Fig S3S-T). Altogether, we conclude that deubiquitination of Shrub and CHMP2B by USP8 is required to block their localization at RCs and subsequent abscissions, allowing the formation of 16-cell germline cysts.

Next, we tested the relevance of ESCRT proteins ubiquitination during complete abscission. We previously showed that Shrub is required for the completion of abscission in germline stem cells (*8*). Indeed, removing one copy of *Shrub* (*Shrub*^{G5}/+) in stem cells was sufficient to block abscission and led to the formation of stem-cysts in 60% of stem cells (Fig 4A). Knocking-down *Usp8* in this context rescued abscission arrest and the formation of stem-cysts, indicating that ubiquitination could also regulate ESCRT-III in GSCs (Fig 4A). To further test this conclusion, we expressed a non-ubiquitinable variant of Shrub (Shrub-KR) in *Shrub*^{G5}/+ GSCs and tested its ability to replace endogenous Shrub (Fig S4A-B). Surprisingly, we found that Shrub-KR and Shrub-WT were equally able to fully rescue stem-cysts phenotypes of *Shrub*^{G5}/+ females (Fig 4B-C). Like Shrub-WT, Shrub-KR localized at RCs and midbodies of *Shrub*^{G5}/+ heterozygous GSC/CB pairs (Fig 4B, S4C). This result indicated that Shrub-KR was still functional, and able to localize properly when one copy of endogenous Shrub remained in GSCs. We speculated that endogenous – and ubiquitinatable- Shrub remaining in *Shrub*^{G5}/+ females could help Shrub-KR to localize and promote complete abscission. In agreement, we could precipitate Shrub-KR and Shrub-WT in *Drosophila* cells, indicating that both proteins could interact physically

(Fig S4D). Importantly, when we removed both copies of *Shrub* in GSCs, we found that Shrub-KR only poorly compensated for the absence of Shrub, while Shrub-WT rescued *Shrub* mutant germline clones (Fig 4D-G). In these non-rescued GSCs, Shrub-KR only formed cytoplasmic aggregates and did not localize at RCs (Fig 4E-F). In the few rescued GSCs, Shrub-KR weakly localized at RCs, indicating that alternative ubiquitin-independent interaction might also be involved in ESCRT-III localization and function during abscission (Fig S4E). Overall, our results show that in both GSCs and germline cysts, USP8 deubiquitinates ESCRT-III proteins to inhibit their accumulation at intercellular bridges (Fig 4H). However, while ESCRT are barely detectable in germline cysts, they accumulate at GSC midbodies, despite the expression of USP8 in both cell types (Fig 4H).

This apparent contradiction could be explained by a major difference in cell cycle length between GSCs and germline cysts. GSCs cycle in 24h and take around 15h to complete abscission (*28, 29*). In contrast, cysts go through 4 rounds of mitosis in 24h, that is 6h for each cycle. In GSCs, we measured a progressive accumulation of ESCRT-III proteins at GSC/CB intercellular bridge during the 15h post-mitosis, while ESCRT-III remained barely detectable in cyst cells (Fig 5A). In contrast, in the absence of *Usp8*, we observed that CHMP2B also accumulated progressively in cyst cells with ectopic abscission (Fig 5A). We also noted that the levels of USP8 varied along the cell cycle, peaking during mitosis (Fig 5B). These observations have led us to propose that in GSCs, ESCRT proteins have time to accumulate to complete abscission before the following mitosis, whereas in cysts, shorter cell cycles and the presence of peak levels of USP8, prevent ESCRT accumulation and by that stabilize incomplete divisions. In this model, the combination of different cell cycle lengths and USP8 accumulation during mitosis is sufficient to explain the switch from complete to incomplete cytokinesis (Fig 5F). To test this model experimentally, we reasoned that lengthening the post-mitotic phase of germline cysts could be sufficient for ESCRT proteins accumulation and completion of cell divisions. We used flies in which the differentiation of germline cysts could be synchronized by the expression of the *bam* gene following a heat-shock (HS) (*11, 30*). At 18h post-HS, the majority of 4-cell cysts in these flies were devoid of ESCRT proteins as in wild type cysts (Fig 5C', D-E left).When we dissected flies 28h post-HS, most cysts had reached the 8-cell stage, yet some were still at the 4-cell stage, and exhibited CHMP2B-GFP at the RCs (Fig 5E middle), some of which were even breaking apart as in *Usp8* mutant cysts. At 38hr post-HS, we observed an increase in the number of 4-cell cysts breaking apart (Fig 5E, right). These results show that when germline cysts were blocked at the 4-cell stage for at least 10h (from 18h to 28h) or 20h (from 18h to 38h), they accumulated ESCRT proteins at ring canals and complete abscission. These cysts also did not enter mitosis nor experience another peak of USP8. These results strongly support our model showing that lengthening the post-mitotic phase of 4-cell cysts, even in a *Usp8* and ESCRT wild type background, is sufficient for ESCRT proteins to accumulate at ring canals and induce ectopic abscission in germline cysts, as in a *Usp8* mutant (Fig 5F).

Collectively, our data demonstrates that ubiquitination of ESCRT-III is critical to regulate the switch between complete and incomplete divisions. We propose a model in which USP8 deubiquitinates ESCRT-III proteins Shrub and CHMP2B, which prevents complete abscission and allows sister cells to remain linked by stabilized cytoplasmic bridges (Fig 4H). Ubiquitination of Shrub and CHMP2B could induce conformational changes similar to other ESCRT-III proteins and modify their ability to form dynamic helices (*27, 31-33*). Alternatively, ubiquitination of CHMP2B and Shrub could modulate their interactions with membrane-associated partners, such as Alix and/or CHMP6, which are known to be important for ESCRT-III recruitment during abscission (*14, 34-36*). Our results also revealed that complete and incomplete abscission are not inherently different in nature. Both GSCs and germline cysts express *Usp8* and several ESCRT-III proteins, despite different outcomes for abscission. We propose that it is mainly the kinetics of abscission, which are different in the two cases (Fig 5F). We have previously shown that GSCs cytokinesis is very sensitive to Shrub concentration (*8*). Here, we show that ubiquitination could be an additional level of regulation of Shrub local concentration. The ratio of ubiquinated vs non-ubiquitinated forms of Shrub could change the kinetics of filament formation. Indeed, we found that removing partially Shrub or CHMP2B was sufficient to rescue the absence of USP8. These strong genetic interactions indicate that the relative amounts of USP8 and ESCRT-III proteins are key to the regulation of complete vs incomplete abscission.

A major question arising from our work is the evolutionary relationship between complete and incomplete division, and whether USP8 played a role in the emergence of one from the other. In the *Drosophila* germline lineage, we observed the most dramatic consequences of *Usp8* loss in germline cysts, where cytokinesis is incomplete, rather than in stem cells with complete cytokinesis. This indicates that USP8 main function is to promote incomplete division and that it seems dispensable for complete cytokinesis. Cyst formation is wildly found in animal germline cells (*37*). In mouse and *Drosophila* females, the formation of cysts allows the transport of organelles and nutrients from sister cells into the future oocytes. In male cysts, stable cytoplasmic bridges are thought to play an important role in sharing X-linked and Y-linked gene products between spermatocytes during their differentiation (*3, 4, 37-40*). Besides germ cells, unicellular organisms such as the choanoflagellates can also form colonies of sister cells by incomplete divisions. Considered as a first step toward multicellularity, these colonies are linked by cytoplasmic bridges strikingly resembling metazoan ring canals (*1, 2*). Since ESCRT-III function in abscission is conserved from archaebacteria to vertebrates (*41*), it will be interesting to investigate if ubiquitination of ESCRT-III plays a role in the emergence of these incomplete divisions.

Acknowledgements

We thank M.O. Fauvarque, S. Goto, F.K. Teixeira, M. Furthauer, P. Thérond, K. Haglund, the Bloomington Stock center, the DSHB for reagents used in this study. We thank Arnaud Echard for discussions and suggestions, and the Huynh lab, M.H. Verlhac, D. St Johnston, and E. Montembault for helpful comments on the manuscript. We are grateful to the Orion Imaging Facility (Collège de France) and BDD Curie Imaging facility. The J.-R.H. lab is supported by CNRS, INSERM, Collège de France, La Fondation pour la Recherche Médicale (FRM) (Equipes FRM DEQ20160334884), Agence Nationale de la Recherche (ANR) (ANR-15-CE13-0001-01, AbsCyStem) and the Bettencourt Schueller Foundation.

References

1. S. R. Fairclough, M. J. Dayel, N. King, Multicellular development in a choanoflagellate. *Curr Biol* **20**, R875-876 (2010).
2. M. J. Dayel *et al.*, Cell differentiation and morphogenesis in the colony-forming choanoflagellate Salpingoeca rosetta. *Dev Biol* **357**, 73-82 (2011).
3. M. E. Pepling, M. de Cuevas, A. C. Spradling, Germline cysts: a conserved phase of germ cell development? *Trends Cell Biol* **9**, 257-262 (1999).
4. K. Haglund, I. P. Nezis, H. Stenmark, Structure and functions of stable intercellular bridges formed by incomplete cytokinesis during development. *Commun Integr Biol* **4**, 1-9 (2011).
5. J. R. Huynh, D. St Johnston, The origin of asymmetry: early polarisation of the Drosophila germline cyst and oocyte. *Curr Biol* **14**, R438-449 (2004).
6. N. Loncle, M. Agromayor, J. Martin-Serrano, D. W. Williams, An ESCRT module is required for neuron pruning. *Sci Rep* **5**, 8461 (2015).
7. J. Mathieu, J. R. Huynh, Monitoring complete and incomplete abscission in the germ line stem cell lineage of Drosophila ovaries. *Methods Cell Biol* **137**, 105-118 (2017).
8. N. R. Matias, J. Mathieu, J. R. Huynh, Abscission is regulated by the ESCRT-III protein shrub in Drosophila germline stem cells. *PLoS Genet* **11**, e1004653 (2015).
9. A. Mukai *et al.*, Balanced ubiquitylation and deubiquitylation of Frizzled regulate cellular responsiveness to Wg/Wnt. *EMBO J* **29**, 2114-2125 (2010).
10. D. McKearin, B. Ohlstein, A role for the Drosophila bag-of-marbles protein in the differentiation of cystoblasts from germline stem cells. *Development* **121**, 2937-2947 (1995).
11. T. Kai, A. Spradling, Differentiating germ cells can revert into functional stem cells in Drosophila melanogaster ovaries. *Nature* **428**, 564-569 (2004).
12. L. Gilboa, R. Lehmann, Repression of primordial germ cell differentiation parallels germ line stem cell maintenance. *Curr Biol* **14**, 981-986 (2004).
13. J. Mathieu *et al.*, Aurora B and cyclin B have opposite effects on the timing of cytokinesis abscission in Drosophila germ cells and in vertebrate somatic cells. *Dev Cell* **26**, 250-265 (2013).
14. A. H. Eikenes *et al.*, ALIX and ESCRT-III coordinately control cytokinetic abscission during germline stem cell division in vivo. *PLoS Genet* **11**, e1004904 (2015).
15. C. G. Sanchez *et al.*, Regulation of Ribosome Biogenesis and Protein Synthesis Controls Germline Stem Cell Differentiation. *Cell Stem Cell* **18**, 276-290 (2016).
16. E. Mizuno *et al.*, Regulation of epidermal growth factor receptor down-regulation by UBPY-mediated deubiquitination at endosomes. *Mol Biol Cell* **16**, 5163-5174 (2005).
17. W. Luo *et al.*, CLOCK deubiquitylation by USP8 inhibits CLK/CYC transcription in Drosophila. *Genes Dev* **26**, 2536-2549 (2012).
18. A. Mukai *et al.*, Dynamic regulation of ubiquitylation and deubiquitylation at the central spindle during cytokinesis. *J Cell Sci* **121**, 1325-1333 (2008).

19. P. E. Row *et al.*, The MIT domain of UBPY constitutes a CHMP binding and endosomal localization signal required for efficient epidermal growth factor receptor degradation. *J Biol Chem* **282**, 30929-30937 (2007).
20. J. Guizetti *et al.*, Cortical constriction during abscission involves helices of ESCRT-III-dependent filaments. *Science* **331**, 1616-1620 (2011).
21. L. Christ, C. Raiborg, E. M. Wenzel, C. Campsteijn, H. Stenmark, Cellular Functions and Molecular Mechanisms of the ESCRT Membrane-Scission Machinery. *Trends Biochem Sci* **42**, 42-56 (2017).
22. J. Schoneberg, I. H. Lee, J. H. Iwasa, J. H. Hurley, Reverse-topology membrane scission by the ESCRT proteins. *Nat Rev Mol Cell Biol* **18**, 5-17 (2017).
23. C. L. Stoten, J. G. Carlton, ESCRT-dependent control of membrane remodelling during cell division. *Semin Cell Dev Biol* **74**, 50-65 (2018).
24. B. Mierzwa, D. W. Gerlich, Cytokinetic abscission: molecular mechanisms and temporal control. *Dev Cell* **31**, 525-538 (2014).
25. E. Nikko, B. Andre, Evidence for a direct role of the Doa4 deubiquitinating enzyme in protein sorting into the MVB pathway. *Traffic* **8**, 566-581 (2007).
26. N. Johnson, M. West, G. Odorizzi, Regulation of yeast ESCRT-III membrane scission activity by the Doa4 ubiquitin hydrolase. *Mol Biol Cell* **28**, 661-672 (2017).
27. X. Crespo-Yanez *et al.*, CHMP1B is a target of USP8/UBPY regulated by ubiquitin during endocytosis. *PLoS Genet* **14**, e1007456 (2018).
28. G. Villa-Fombuena, M. Lobo-Pecellin, M. Marin-Menguiano, P. Rojas-Rios, A. Gonzalez-Reyes, Live imaging of the Drosophila ovarian niche shows spectrosome and centrosome dynamics during asymmetric germline stem cell division. *Development* **148**, (2021).
29. L. X. Morris, A. C. Spradling, Long-term live imaging provides new insight into stem cell regulation and germline-soma coordination in the Drosophila ovary. *Development* **138**, 2207-2215 (2011).
30. B. Ohlstein, D. McKearin, Ectopic expression of the Drosophila Bam protein eliminates oogenic germline stem cells. *Development* **124**, 3651*3662 (1997).
31. I. Goliand *et al.*, Resolving ESCRT-III Spirals at the Intercellular Bridge of Dividing Cells Using 3D STORM. *Cell Rep* **24**, 1756-1764 (2018).
32. B. E. Mierzwa *et al.*, Dynamic subunit turnover in ESCRT-III assemblies is regulated by Vps4 to mediate membrane remodelling during cytokinesis. *Nat Cell Biol* **19**, 787-798 (2017).
33. A. K. Pfitzner *et al.*, An ESCRT-III Polymerization Sequence Drives Membrane Deformation and Fission. *Cell* **182**, 1140-1155 e1118 (2020).
34. J. G. Carlton, J. Martin-Serrano, Parallels between cytokinesis and retroviral budding: a role for the ESCRT machinery. *Science* **316**, 1908-1912 (2007).
35. L. Christ *et al.*, ALIX and ESCRT-I/II function as parallel ESCRT-III recruiters in cytokinetic abscission. *J Cell Biol* **212**, 499-513 (2016).
36. C. Addi *et al.*, The Flemmingsome reveals an ESCRT-to-membrane coupling via ALIX/syntenin/syndecan-4 required for completion of cytokinesis. *Nat Commun* **11**, 1941 (2020).
37. K. Lu, L. Jensen, L. Lei, Y. M. Yamashita, Stay Connected: A Germ Cell Strategy. *Trends Genet* **33**, 971-978 (2017).
38. J. R. Huynh, in *Cell-cell Channels* F. Baluska, D. Volkmann, P. W. Barlow, Eds. (Springer-Landes Biosciences 2005).
39. R. S. Kaufman *et al.*, Drosophila sperm development and intercellular cytoplasm sharing through ring canals do not require an intact fusome. *Development*, (2020).
40. L. Lei, A. Spradling, Mouse oocytes differentiate through organelle enrichment from sister cyst germ cells. *Science* **352**, 95-99 (2016).
41. G. Tarrason Risa *et al.*, The proteasome controls ESCRT-III-mediated cell division in an archaeon. *Science* **369**, (2020).

Figure legends

Figure 1: USP8 is necessary and sufficient to block abscission in the germline lineage

(A) Top: Schematic representation of a female ovariole showing the germarium where germline cell divide, and an egg chamber. Bottom: schematic representation of the cell lineage of the germline stem cell (GSC). The GSC self-renews and gives rise, after complete cytokinesis, to another GSC and a cystoblast (CB). The CB divides four times synchronously with incomplete cytokinesis, forming subsequently a 2-cell cyst, a 4-cell cyst, an 8-cell cyst and a 16-cell cyst. (B) Schematic representation of the mitotic region of the germarium. At the end of mitosis, GSC are connected to their daughter CB through a ring canal (RC) (GSC #1) and later by a midbody (MB) (GSC #2). After complete cytokinesis, the GSC and CB are fully separated (GSC #3). The fusome (red) links the GSC and the CB before abscission, and also passes through all the RC of the germline cysts. Cap cells are represented in light grey, the terminal filament cell is in dark grey. (C-F) Confocal images of fixed ovarioles (C, E) and germaria (D, F) of females expressing *shRNA-w* or *shRNA-Usp8* (P{TRiP.HMS01941}attP2) under the control of *nos-GAL4* driver. D'and F' are close-up images of the cysts framed in D and F. Dotted lines surround germline cysts. The white arrow indicates the ectopic midbody (MB) of the breaking cyst. Scale bar: 20 μm in C, E and 10 μm in D, F. (G) Fraction of germaria exhibiting at least one breaking cyst. n indicates the total number of germaria analyzed. (H-I) Confocal images of fixed germaria from a female with $Usp8^{KO}$ GLC (RFP negative cells) expressing *bam-GFP* under the control of *bam* promoter. In H, a RFP positive 8CC shows control Bam-GFP level; in I, a RFP negative breaking 4CC with normal Bam-GFP. Scale bar: 10 μm. I' is a close-up view of the cyst framed in I. Dotted lines surround a breaking germline cyst. The white arrow indicates the ectopic midbody (MB) of the breaking cyst. (J-K,M) Confocal images of a fixed ovariole (J) and germarium (K,M) from females expressing *Usp8-WT* (J-K) or *Usp8-C572A* (M) under the control of *nosG4-GAL4* driver. Dotted lines surround a stem-cyst that originates from a GSC. Scale bar: 20 μm in I and 10 μm in J. (L) Fraction of germaria exhibiting a stem-cyst. n indicates the total number of germaria analyzed.

Figure 2: The deubiquitinating activity of USP8 is essential for its function in germline cysts

(A) Scheme of the V5 tagged variants of USP8 proteins. (B) Fraction of 4 cell-cysts and 8 cell-cysts exhibiting a breaking phenotype. P values (p) are indicated and derived from Chi square tests. n represent the numbers of cysts analyzed. (C, D, E) Confocal images of germaria of females with $Usp8^{KO}$ GLC (RFP negative cells). C', D', E' are close-up views of the cysts framed in C, D, E. Dotted lines surround germline cysts. White arrows indicate the ectopic MBs, red arrows indicate RCs. (F-G) Confocal images of a germaria expressing *shRNA-w* (F) or *shRNA-Usp8* (G, P{TRiP.HMS01941}attP2) under the control of *nos-GAL4* driver stained with α-Ubiquitin (Ubi) and α-Spectrin. F'and F'' are close up views of the GSC/CB pair framed in F; G' and G" are close up views of the breaking 4CC framed in G. White arrows indicate the MB between the GSC and the CB in F, and

the MB of the breaking 4CC in G. Scale bar: 10 μm. (H-I) Confocal images of germaria expressing GFP tagged USP8 from the endogenous locus. H'and I' are close-up of the cells framed in H and I. Dotted lines surround a GSC and its daughter CB (H'), and a germline cyst (I'). The white arrow indicates the MB between the GSC and the CB in G', and the red arrow indicates the central ring canal in H'. Scale bar: 10 μm.

Figure 3: USP8 regulates CHMP2B and Shrub ubiquitination levels and localization

(A) Immunoblots of Input (In, 1/20 of the IP) or Immunoprecipitated (IP) ESCRT-III proteins from S2 cells transfected with ESCRT-HA and V5-tagged USP8 variants. Membranes were blotted with α-V5 antibody. Three ESCRT-III were tested: CHMP1, CHMP2B and Shrub. Immunoblot representative of 3 experiments. (B) Immunoblots of Input (In, 1/20 of the IP) or Immunoprecipitated (IP) ubiquitinated proteins from S2 cells transfected with ESCRT-HA, His-tagged Ubiquitin, and V5-tagged USP8 variants. Membranes were blotted with α-HA antibody, to reveal ubiquitinated ESCRT-III. Three ESCRT-III were tested: CHMP1, CHMP2B and Shrub. Immunoblot representative of 3 experiments. The red frame highlights the experiment showing that USP8 transfection is sufficient to abolish CHMP2B and Shrub ubiquitination. (C-D) Confocal images of fixed germaria of females expressing *Shrub-HA* under the control of *nos-Gal4*. C', D' are close up images of the regions framed in C and D. A GSC/CB pair (C') and an 8CC (D') are surrounded by dotted lines. The white arrow in C and C' indicates the MB between the GSC and the CB. Shrub-HA is not detected in the 8CC. Scale bar: 10 μm. (E) Confocal images of a fixed germarium of a female expressing *Shrub-HA* under the control of *nos-Gal4* with $Usp8^{KO}$ GLC (RFP negative cells). E', E" and E'" are close up of the regions framed in C, D, E. The white arrow indicates the ectopic MB of the breaking 4CC framed in E, the red arrows indicate ectopic Shrub-HA at the RCs of the mutant 4CC. Scale bar: 10 μm. (F-G) Confocal images of fixed germaria of females expressing *shRNA-Usp8* (P{TRiP.HMS01941}attP2) in a WT (F) or $shrb^{G5}$/+ (G) background. Cysts are surrounded by dotted lines: in (F) a breaking 4CC, in (G), a non-breaking 8CC. White arrow indicates the MB of the breaking 4CC. Scale bar: 10 μm (H) Fraction of 4CC exhibiting a breaking phenotype. P values (p) are derived from Chi Square tests. n represent the numbers of cysts analyzed. (I-J) Confocal images of fixed ovarioles of females expressing *shRNA-Usp8* (P{TRiP.HMS01941}attP2) in a WT (I) or $shrb^{G5}$/+ (J) background. The number of nuclei of some ovarioles are indicated. Scale bar: 20 μm.

Figure 4: Ubiquitination of Shrub is essential to promote abscission in the GSCs

(A) Fraction of GSCs exhibiting a stem-cyst or polyploïd phenotype. P values (p) are derived from Chi Square tests. n represents the numbers of GSC analyzed. (B) Confocal image of a fixed germarium from a $shrb^{G5}$/+ female expressing *Shrb-KR-HA*. The dotted line surrounds a GSC/CB pair. The red arrow indicates the Shrb-KR-HA positive RC. Such strong staining was observed in all GSC/CB pair (n>30).

Scale bar: 10 μm (C) Fraction of GSCs with a stem cyst or polyploid phenotype. n represent the numbers of GSC analyzed. (D-F) Confocal images of fixed germaria with *shrb*^{G5} GLC (GFP negative) expressing *Shrb-WT-HA* (E), *Shrb-KR-HA* (F) or no transgene (D). Dotted lines surround a GSC/CB pair (E) or stem-cysts (D, F). White arrow indicates the MB positive for Shrb-WT-HA. Scale bar:10 μm (G) Fraction of GSCs with a stem cyst or polyploid phenotype. P values (p) are derived from Chi Square tests. ns: not significant (p=0.01). n represents the number of cysts analyzed. (H) USP8 deubiquitination of ESCRT-III inhibits their localization and/or activity at the abscission site. In WT GSCs, ubiquitinated ESCRT-III promote constriction of the RC and abscission. In germline cysts, USP8 activity is required to deubiquitinate ESCRT-III, blocking their enrichment at the RC, and causing incomplete abscission.

Figure 5: Different kinetics of ESCRT-III accumulation at intercellular bridges in GSCs and germline cysts.

(A) Fluorescence intensity (arbitrary unit A. U.) of CHMP2B-GFP at the ring canal (pre-MB) or the MB of GSC, and at the central RC of cysts (2CC, 4CC, 8CC) in control (green) or *sh-Usp8* (red, P{TRiP.HMS01941}attP2) expressing flies. P values (p) between control and sh-RNA expressing flies are derived from Mann-Witney tests. (B) Fluorescence intensity (arbitrary unit A. U.) of USP8-GFP at the ring canal (pre-MB) or the MB of GSC, and at the central RC of cysts (2CC, 4CC, 8CC and 16CC) in *Usp8*^{KI} flies in interphase (black) or mitosis (orange). P values (p) between interphase and mitosis are derived from Mann-Witney tests. (C-C'') Confocal images of a fixed germaria from *bam*$^{\Delta 86}$ females expressing *CHMP2B-GFP* from endogenous promoter and *bam* under the control of heat shock (HS) driver. Females were dissected without HS (C, no HS), or 18 (C') or 38hrs (C'') after adult HS. (D-E) Confocal images and schemes of fusomes (stained for α-spectrin, red) in germaria of WT females expressing *CHMP2B-GFP* (D) or of *bam*$^{\Delta 86}$ females expressing *CHMP2B-GFP* and *bam* under the control of heat shock (HS) driver (E). Time after HS are indicated on the dark arrow between (D) and (E). In (D), the fusome expends between the increasing number of cells as the cysts grow. In (E), 4CC are observed at HS+18hrs (left). CHMP2B-GFP is then observed at the RCs (red arrow) of a 4CC (middle), and the central RC of a 4CC breaks into a MB (white arrow) at HS+38hrs (right). (F) Schematic model of ESCRT levels over time in the germarium. The GSC has a 24hrs cell cycle. Abscission between the newly formed GSC and its daughter CB occurs late in the cell cycle, before the next mitosis, and so that the GSC/CB pair never experiences a USP8 peak. During this long period, the GSC/CB RC therefore accumulates ESCRT, reaching a high level allowing abscission. The CB becomes a 16CC in 24hrs, therefore each cycle lasts only 6hrs, leaving much less time to accumulate ESCRT at RC at each cycle. In addition, USP8 levels at the RC in the cyst peak at each mitosis (orange bars) and remove (or block the dynamic recruitement of) ESCRTs at the RCs. We propose that short cell cycle duration combined with USP8 peaks in mitosis are responsible for the low levels of ESCRT at cysts RC,

and absence of abscission. When USP8 is absent (red), ESCRT levels increase at each cyst cycle, allowing abscission.

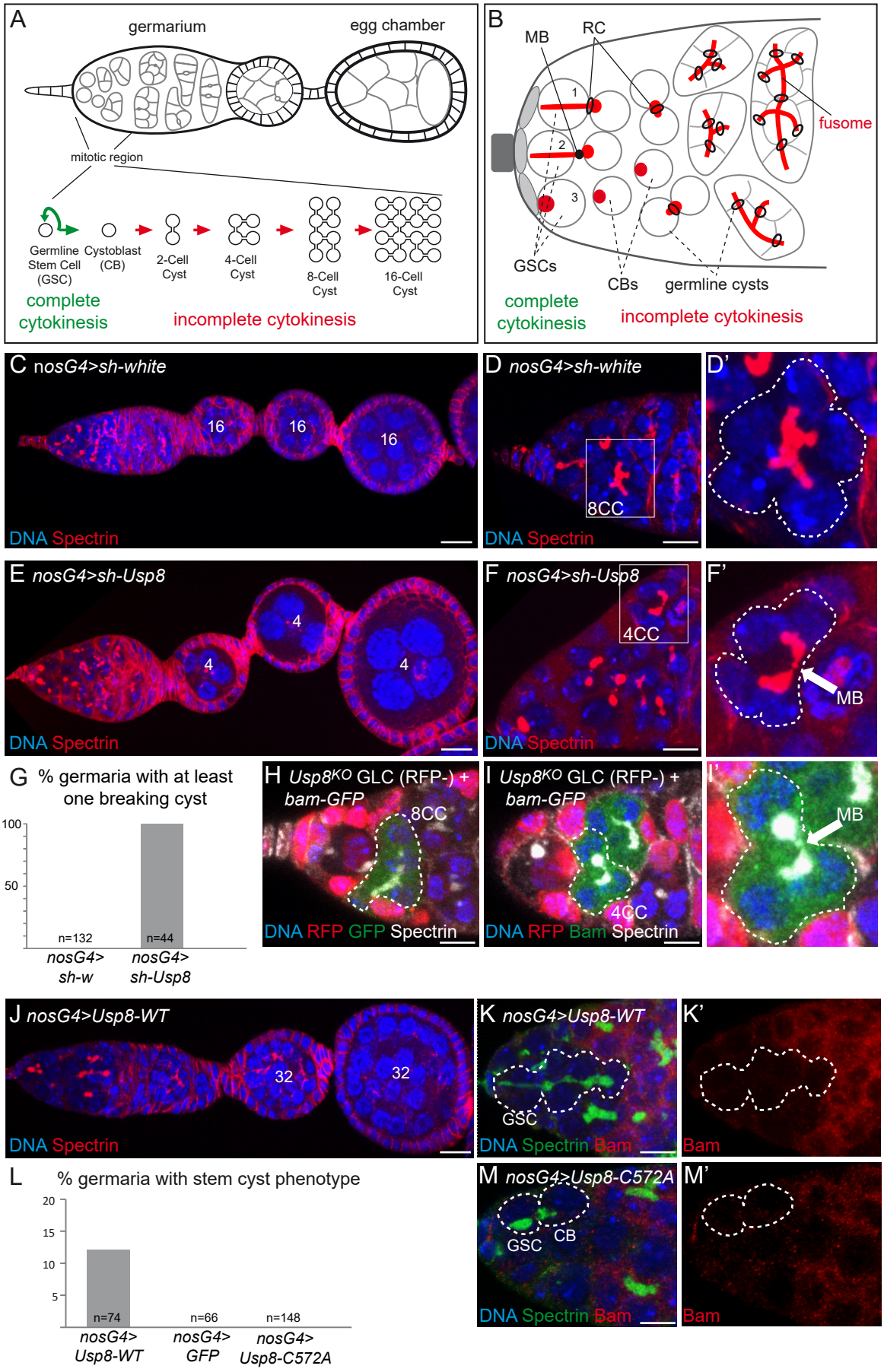
A
germarium
egg chamber
mitotic region
Germline Stem Cell (GSC)
Cystoblast (CB)
2-Cell Cyst
4-Cell Cyst
8-Cell Cyst
16-Cell Cyst
complete cytokinesis
incomplete cytokinesis
B
MB
RC
fusome
GSCs
CBs
germline cysts
complete cytokinesis
incomplete cytokinesis
C nosG4>sh-white
16
16
16
DNA Spectrin
D nosG4>sh-white
8CC
DNA Spectrin
D'
E nosG4>sh-Usp8
4
4
4
DNA Spectrin
F nosG4>sh-Usp8
4CC
DNA Spectrin
F'
MB
G % germaria with at least one breaking cyst
100
50
n=132
n=44
nosG4> sh-w
nosG4> sh-Usp8
H Usp8KO GLC (RFP-) + bam-GFP
8CC
DNA RFP GFP Spectrin
I Usp8KO GLC (RFP-) + bam-GFP
4CC
DNA RFP Bam Spectrin
I'
MB
J nosG4>Usp8-WT
32
32
DNA Spectrin
K nosG4>Usp8-WT
GSC
DNA Spectrin Bam
K'
Bam
L % germaria with stem cyst phenotype
20
15
10
5
n=74
n=66
n=148
nosG4> Usp8-WT
nosG4> GFP
nosG4> Usp8-C572A
M nosG4>Usp8-C572A
GSC
CB
DNA Spectrin Bam
M'
Bam

Figure 1

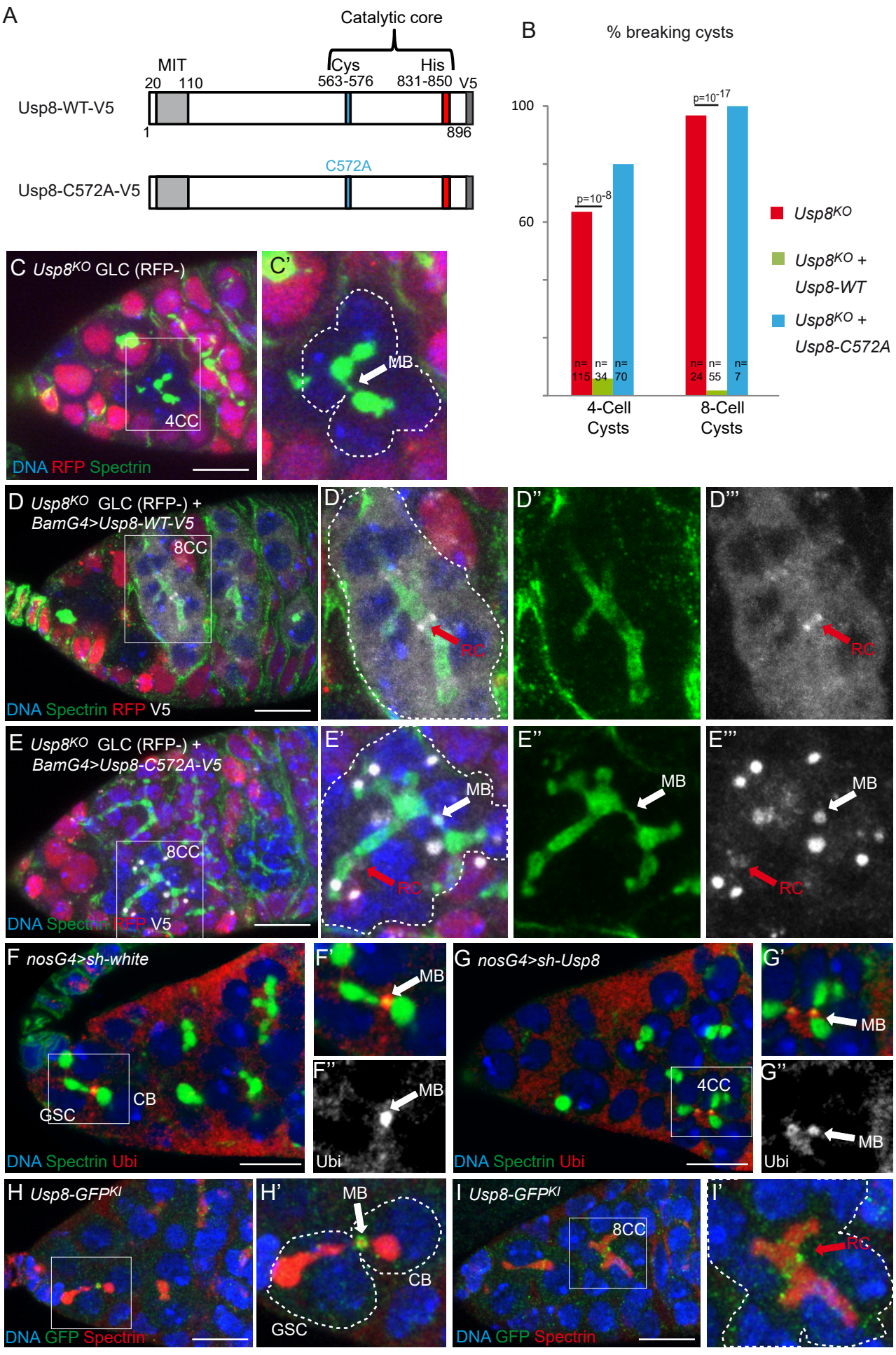
A
Catalytic core
MIT
Cys
His
20
110
563-576
831-850
V5
Usp8-WT-V5
1
896
C572A
Usp8-C572A-V5
B
% breaking cysts
100
60
p=10-8
p=10-17
n= 115
n= 34
n= 70
n= 24
n= 55
n= 7
4-Cell Cysts
8-Cell Cysts
Usp8KO
Usp8KO + Usp8-WT
Usp8KO + Usp8-C572A
C Usp8KO GLC (RFP-)
C'
MB
4CC
DNA RFP Spectrin
D Usp8KO GLC (RFP-) + BamG4>Usp8-WT-V5
D'
D''
D'''
8CC
RC
DNA Spectrin RFP V5
E Usp8KO GLC (RFP-) + BamG4>Usp8-C572A-V5
E'
E''
E'''
MB
RC
8CC
DNA Spectrin RFP V5
F nosG4>sh-white
F'
F''
G nosG4>sh-Usp8
G'
G''
CB
GSC
4CC
DNA Spectrin Ubi
Ubi
H Usp8-GFPKI
H'
I Usp8-GFPKI
I'
CB
GSC
8CC
DNA GFP Spectrin

Figure 2

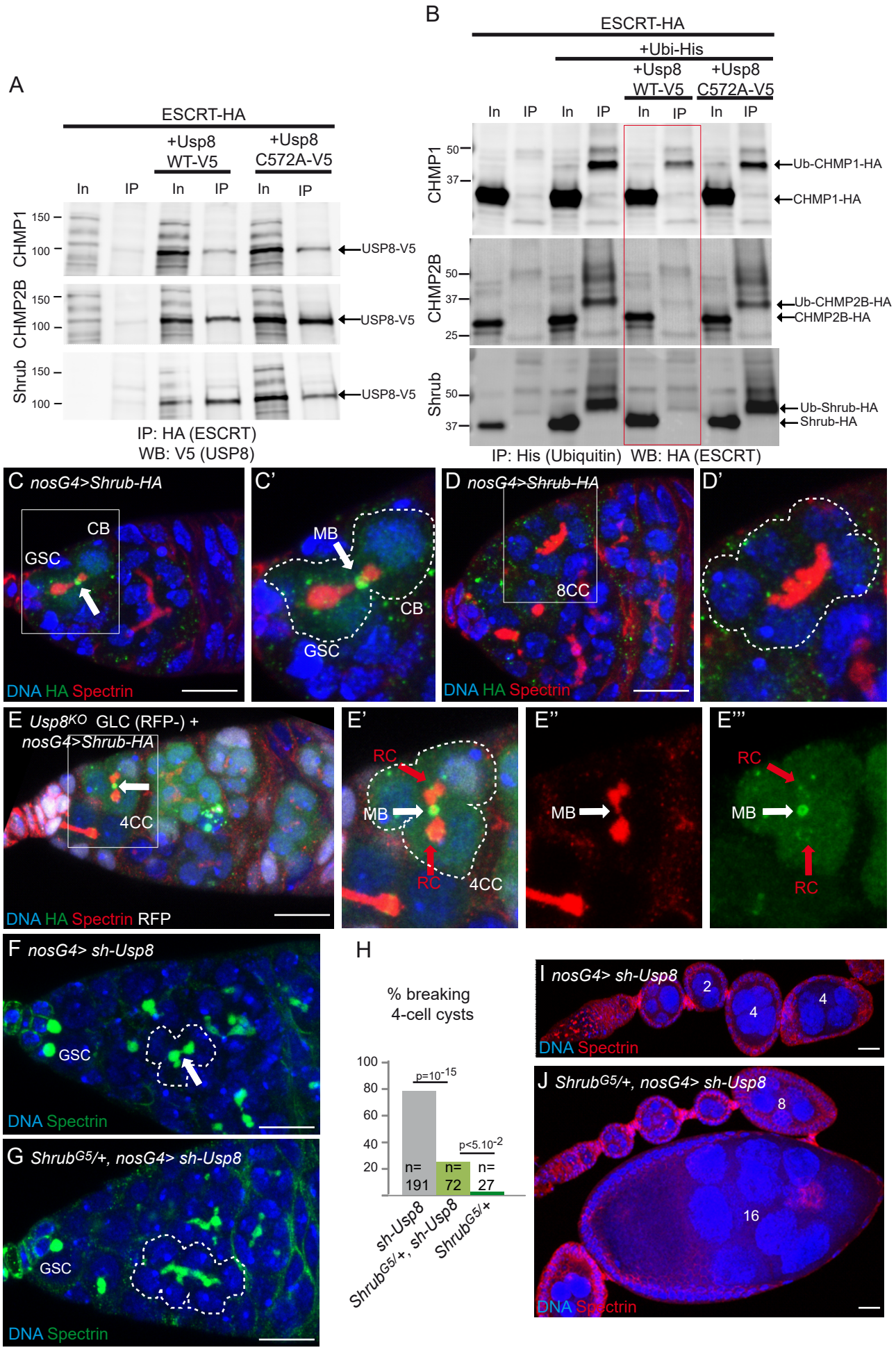
A
ESCRT-HA
+Usp8 WT-V5
+Usp8 C572A-V5
In IP In IP In IP
CHMP1
CHMP2B
Shrub
150
100
USP8-V5
IP: HA (ESCRT)
WB: V5 (USP8)
B
ESCRT-HA
+Ubi-His
+Usp8 WT-V5
+Usp8 C572A-V5
In IP In IP In IP In IP
CHMP1
CHMP2B
Shrub
50
37
25
Ub-CHMP1-HA
CHMP1-HA
Ub-CHMP2B-HA
CHMP2B-HA
Ub-Shrub-HA
Shrub-HA
IP: His (Ubiquitin) WB: HA (ESCRT)
C nosG4>Shrub-HA
CB
GSC
DNA HA Spectrin
C'
MB
CB
GSC
D nosG4>Shrub-HA
8CC
DNA HA Spectrin
D'
E Usp8KO GLC (RFP-) + nosG4>Shrub-HA
4CC
DNA HA Spectrin RFP
E'
RC
MB
RC
4CC
E''
MB
E'''
RC
MB
RC
F nosG4> sh-Usp8
GSC
DNA Spectrin
G ShrubG5/+, nosG4> sh-Usp8
GSC
DNA Spectrin
H
% breaking 4-cell cysts
100
80
60
40
20
p=10-15
p<5.10-2
n= 191
n= 72
n= 27
sh-Usp8
ShrubG5/+, sh-Usp8
ShrubG5/+
I nosG4> sh-Usp8
2
4
4
DNA Spectrin
J ShrubG5/+, nosG4> sh-Usp8
8
16
DNA Spectrin

Figure 3

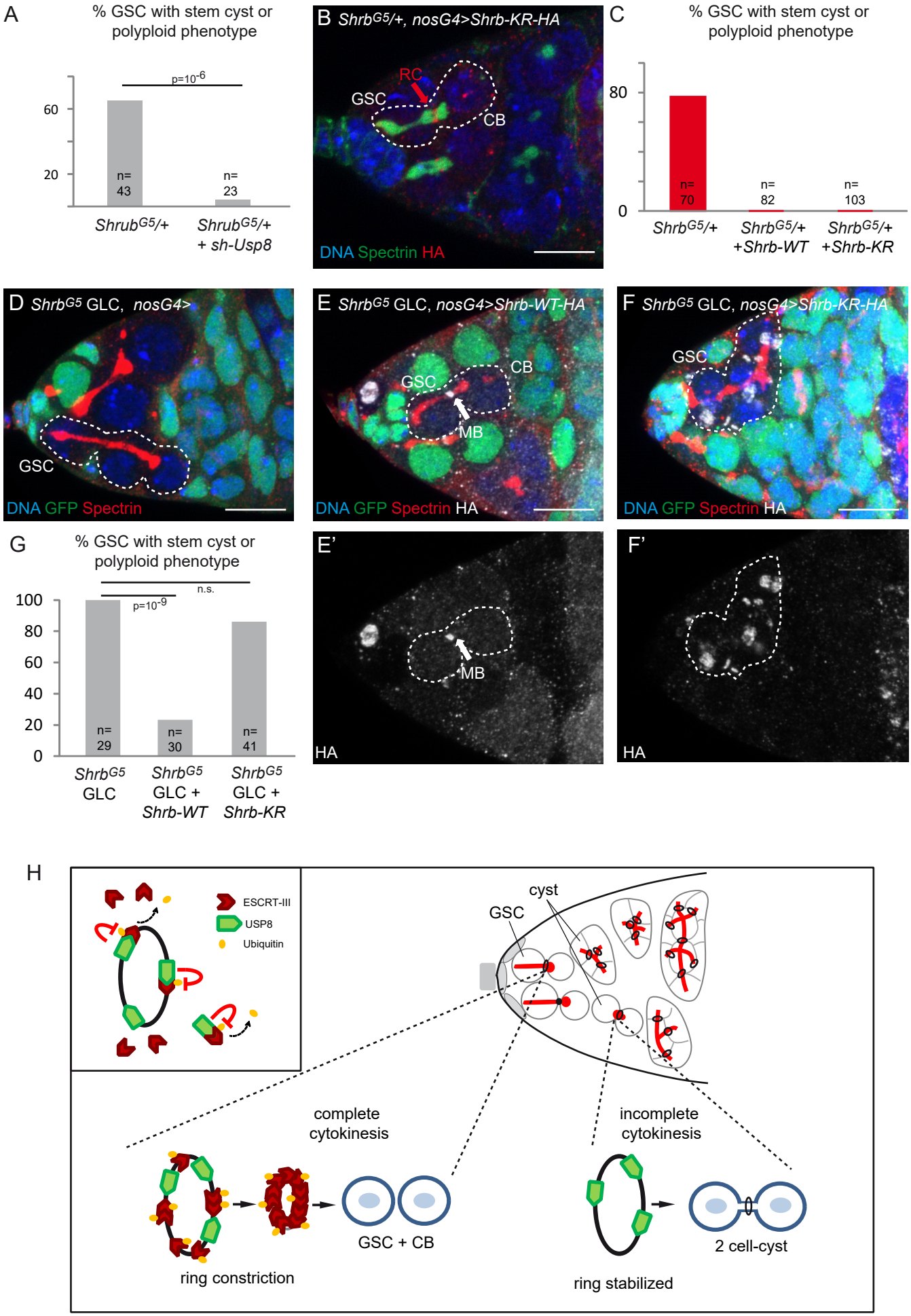
A
% GSC with stem cyst or polyploid phenotype
p=10-6
60
20
n= 43
n= 23
Shrub G5/+
Shrub G5/+ + sh-Usp8
B Shrb G5/+, nosG4>Shrb-KR-HA
RC
GSC
CB
DNA Spectrin HA
C
% GSC with stem cyst or polyploid phenotype
80
0
n= 70
n= 82
n= 103
Shrb G5/+
Shrb G5/+ +Shrb-WT
Shrb G5/+ +Shrb-KR
D Shrb G5 GLC, nosG4>
GSC
DNA GFP Spectrin
E Shrb G5 GLC, nosG4>Shrb-WT-HA
CB
GSC
MB
DNA GFP Spectrin HA
F Shrb G5 GLC, nosG4>Shrb-KR-HA
GSC
DNA GFP Spectrin HA
G
% GSC with stem cyst or polyploid phenotype
n.s.
p=10-9
100
80
60
40
20
0
n= 29
n= 30
n= 41
Shrb G5 GLC
Shrb G5 GLC + Shrb-WT
Shrb G5 GLC + Shrb-KR
E'
MB
HA
F'
HA
H
ESCRT-III
USP8
Ubiquitin
cyst
GSC
complete cytokinesis
incomplete cytokinesis
GSC + CB
2 cell-cyst
ring constriction
ring stabilized

Figure 4

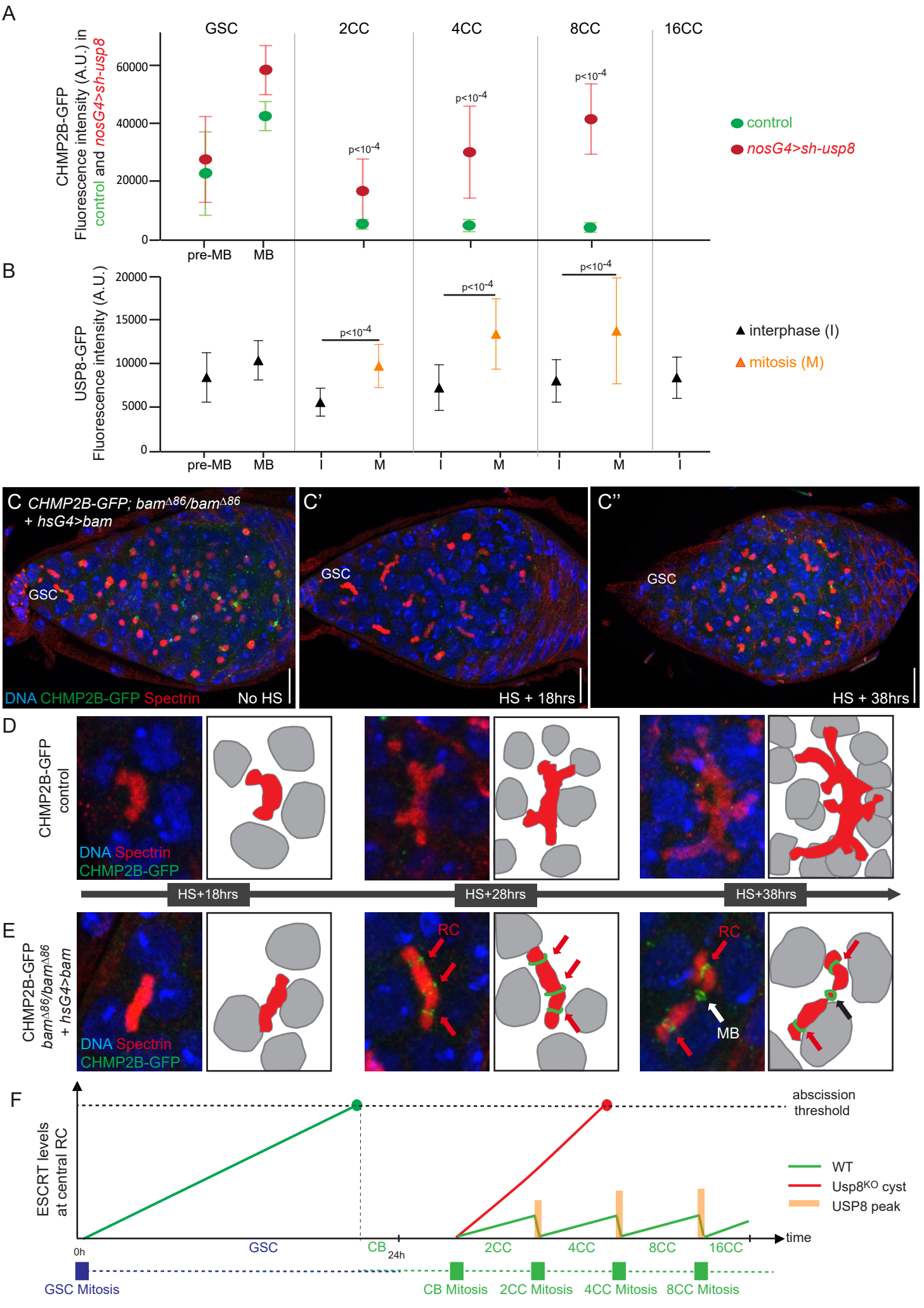
A
GSC
2CC
4CC
8CC
16CC
CHMP2B-GFP
Fluorescence intensity (A.U.) in
control and nosG4>sh-usp8
60000
40000
20000
0
p<10-4
pre-MB
MB
control
nosG4>sh-usp8
B
USP8-GFP
Fluorescence intensity (A.U.)
20000
15000
10000
5000
0
I
M
interphase (I)
mitosis (M)
C CHMP2B-GFP; bamΔ86/bamΔ86
+ hsG4>bam
C'
C''
GSC
DNA CHMP2B-GFP Spectrin
No HS
HS + 18hrs
HS + 38hrs
D
CHMP2B-GFP
control
DNA Spectrin
CHMP2B-GFP
HS+18hrs
HS+28hrs
HS+38hrs
E
CHMP2B-GFP
bamΔ86/bamΔ86
+ hsG4>bam
RC
MB
F
ESCRT levels
at central RC
abscission
threshold
WT
Usp8KO cyst
USP8 peak
time
0h
GSC
CB
24h
2CC
4CC
8CC
16CC
GSC Mitosis
CB Mitosis
2CC Mitosis
4CC Mitosis
8CC Mitosis

Figure 5

Science
AAAS

Supplementary Materials for

Deubiquitinase USP8 targets ESCRT-III to promote incomplete cell division

Juliette Mathieu, Pascale Michel-Hissier, Virginie Boucherit and Jean-René Huynh

Correspondence to: jean-rene.huynh@college-de-france.fr and Juliette.mathieu@college-de-france.fr

This PDF file includes:

Materials and Methods
Supplementary Text
Figs. S1 to S4
Captions for Movies S1 to S6
References
Table of genotypes

Other Supplementary Materials for this manuscript include the following:

Movies S1 to S6

Materials and Methods

Fly stocks and genetics

Fly stocks were grown under standard conditions. *Drosophila* stocks used in this study were: *nos-GAL4* (*1*), *bam-GAL4* (*2*), *bamP-bamGFP* (*3*), *FRT42, shrb^{G5}* (*4*), *UASp-tubulin-PA-GFP* (*5*), *UASp-par1-GFP* (*6*), *Usp8^{KO}* (*7*), *bam$^{\Delta 86}$* (*8*), *hs-Bam (9)*, *alix^{1}* (*10*), *CHMP2B-GFP* (PBac{fTRG00825.sfGFP-TVPTBF}VK00002 / VDRCv318679) (*11*), *Rab5-EYFP* (TI{TI}Rab5[EYFP], BL62543), *Rab7-EYFP* (TI{TI}Rab7[EYFP], BL62545), *trafic-jam-GAL4* (P{tj-GAL4.U} (*12*), TRIP lines allowing shRNA expression (*13*) directed against *white* (P{TRiP.GL00094}attP2 / BL35573), *Usp8* (P{TRiP.HMS01941}attP2 / BL39022 and P{TRiP.HMS01898}attP40 / BL38982), *CHMP2B* (P{TRiP.HMS01844}attP40 / BL38375), and *Bam* (P{TRiP.HMS00029}attP2, BL33631).

Overexpression experiments were performed using the GAL4/UASp system (*14*) with the *nanos-GAL4-VP16* or the *bam-GAL4* drivers. Recombinants were obtained by standard genetic procedures. The germline clones were generated using the FLP/FRT technique (*15*) (*16*) using *hsFLP* alone or recombined with *nos-GAL4*, and a *nls-GFP* or RFP recombined onto *FRT42D*, or *FRT82B*. *Usp8* GLC clones were induced by heat-shocking second or third instar larvae at 37°C for 2 hours, females were dissected 1-2 days after eclosion. *Shrb^{G5}* GLC were induced by heat-shocking adult females at 37°C for 2 hours, females were dissected 4 days after HS. Rescue of *bam$^{\Delta 86}$* mutant females by *hs-bam* was performed by heat-shocking 1- or 2-days old females for 2 hrs at 37°C. Females were then transfered in vials with fresh yeast at 25°C and dissected after 18, 28, 38 and 48hrs.

For the genetic screen aiming to identify genes involved in germline cysts formation, a collection of 34 sh-RNA lines were crossed with *nos-Gal4* driver. Lines were chosen on their potential ability to affect the abscission machinery (BioGrid datas available on FlyBase). Female progenies were dissected, ovaries were stained with Hoechst and analyzed at the epifluorescence microscope. We screened for egg chambers made of 8 or less nuclei and retained these lines for further investigations. Apart from the 2 lines directed against *Usp8* and described in this manuscript, we only identified sh-RNA directed against *Cdk2* in this screen.

Cell culture and transfection

Drosophila S2 cells (Thermo Fisher Scientific) were cultured at 25°C in Schneider's drosophila medium (Thermo Fisher Scientic) supplemented with 10% FBS + 1% Streptomycin/Penicillin. Transfection of Drosophila S2 cells were performed using Effectene transfection Reagent (Qiagen)

according to Manufacturer's instructions. Cells were transfected by 1µg of DNA for 48h before immunoprecipitation.

Molecular Biology: Constructs for transgenic flies

To generate *pUASp-Usp8-V5* and *pUASp-Usp8-C572A-V5*, several steps were conducted. First, we generated a *pFLC1: Usp8-V5* vector: 2 primers containing the V5 tag were annealed, and subsequently inserted by SLIC technology into pFLC1: RH33842 (BDGP clone for *Usp8*) digested by AccI. F:5'**CCCATGCAGGTGCCTCT**GGGTAAGCCTATCCCTAAC**CCTCTCCTCGGT** 3' and R:5'**GGAAACCGAGCGAAGCGTTTA**CGTAGAATCGAG**ACCGAGGAGAGGGTTA** 3'. The underlined region encodes V5 tag, the bold underlined the annealed region. The bold region of For primer correspond to the 3' end of *Usp8* CDS. The bold region of Rev primer corresponds to a STOP codon and the 5' of *Usp8* 3'UTR.

Site directed mutagenesis was then achieved on methylated *pFLC1:Usp8-V5* using the oligos F: 5'TGAAGAATCTGGGCAACACCGCCTATATGAACAG3' and R: 5'GGTGTTGCCCAGATTCTTCAGTCCAGTCAG3' according to manufacturer's instruction (Gene tailor, Invitrogen), to generate *pFLC1-Usp8-C572A-V5*.

To generate *pUASp-Usp8-V5* and *pUASp-Usp8-C572A-V5*, the previous plasmids were used as templates to amplify (*Usp8* CDS + 3'UTR) which were cloned by SLIC technology into pUASp-attB (DGRC 1358) digested by BamHI. The oligos used were the following: F: 5'GCCGCATAGGCCACTAGTGGATCTGGATCGATAAATTTCATGCAAAATAACAAATG 3' and R: 5'CGTTCGAGGTCGACTCTAGAGGATCAACTATAGTCCCGCATACACAGGCGTATATG3'. Transgenesis was performed by Bestgene Inc at the attP16 site.

To generate endogenously GFP tagged Ubpy ($Usp8^{KI}$), the CRISPR/Cas9 technology was used as in (*17*). Two short-guide RNAs (sgRNAs) were cloned into the pU6B-sgRNA-vector (Adgene 49410) digested by BbsI after annealing of two pairs of oligonucleotides: for the first short-guide RNA: 5' AAACATGCAGGTGCCTCTGAAGA3' and 5'GTCGTCTACAGAGGCACCTGCAT3'; for the second short-guide RNA: 5'AAACTGCAGGTGCCTCTGTAGAC3' and 5'GTCGCGTCTACAGAGGCACCTGC3'. The homology sequences HR1 and HR2, flanking the sgRNA targeting sequences were cloned by SLIC technology into a homologous recombination vector harboring a *hs-miniwhite* cassette flanked by *loxP* sites and a GFP sequence for tagging (p936) to generate a C-terminal tagged USP8 protein. HR1 was amplified with the primers F:

5’TATGGGGTGTCGCCCTTCGGGTCTCTAGTTCGGACAAATACAAGAATTACATCAGC3’ and R:
5’ACTGCCTGAAGAACCGCTGGACCCCGAACTCTGCATGGGTGGCAGCCAGGTGTAGA3’. HR2 was amplified with the primers: F:
5’TCCGGAAGTGGTAGCTCAGGGTCTAGTGGAGTGCCTCTGTAGACGCTTCGCTCGGT3’ and R:
5’GCCCTTGAACTCGATTGACGCTCTTCGTCCCCGGCAGATTCATGGCGGGCAGATGA3’. A mix of 50 μg of donor vector, and 25 μg of each guide vector was injected by Bestgene in Cas9 expressing flies (M{vas-Cas9.RFP-}, BL55821). The mini-white selection cassette was then excised by Cre mediated recombination.

To generate endogenously GFP tagged Shrub (*Shrb*^{KI}), a similar strategy was used. The homology sequences HR1 and HR2, flanking the sgRNA targeting sequences were cloned by SLIC technology into a homologous recombination vector harboring a *hs-miniwhite* cassette flanked by *loxP* sites and a GFP sequence for tagging (p935) to generate a N-terminal tagged Shrub protein. The oligonucleotides used to generate the short-guide RNAs were the following: For the first short guide: 5’GTCGTCAGCCAGGATGAGTTTCTT3’ and 5’AAACAAGAAACTCATCCTGGCTGA3’; and for the second short guide: 5’GTCGCTTCCCGAAGAAACTCATCC3’ and 5’AAACGGATGAGTTTCTTCGGGAAG3’. The homology sequences HR1 and HR2 were amplified with the following primers: For HR1:
F:5’CCCGGGCTAATTATGGGGTGTCGCCCTTGGGGACCTTGACTTGGAGCGAACTCTC3’ and R:
5’CCCGGTGAACAGCTCCTCGCCCTTGCTCACCATCCTGGCTGATCTGTTTTTTCACCCG3’; for HR2: F:
5’AGTTCGGGGTCCAGCGGTTCTTCAGGCAGTAGTTTCTTCGGGAAGATGTTCGGCGG3’ and R:
5’GCCCTTGAACTCGATTGACGCTCTTCGACTGGGCAAATCTTCTGTGGGTGCTTCTG3’. A mix of 50 μg of donor vector, and 25 μg of each guide vector was injected by Bestgene in Cas9 expressing flies (M{vas-Cas9.RFP-}, BL55821). The mini-white selection cassette was then excised by Cre mediated recombination.

To generate *pUASp-attB-shrb-HA* and *pUASp-attB-shrbKR-HA*. Oligonicleotides 5'CCACTAGTGGATCTGGATCCATGTACCCATACGATGTTCCAGATTACGCTTAA3' and 5'CGTTCGAGGTCGACTCTAGATTAAGCGTAATCTGGAACATCGTATGGGTACAT3' were annealed and inserted by SLIC technology into *pUASp-attB* digested by BamHI and XhoI to generate *pUASp-attB-HA*. *Shrub* CDS was then amplified on the clone GH13992 (DGRC) with the following primers: For: 5'CGCCCGGGGATCAGATCCGCGGCCGCATGAGTTTCTTCGGGAAGAT3' and Rev: 5'GGAACATCGTATGGGTACATGGATCCGTTGGACCAGGATAAAAGCT3'and inserted upstream of the HA tag into pUASp-attB-HA digested by BamHI by SLIC technology.
To generate *pUASp-attB-Shrub-KR-HA*, a vector containing Shrub mutated for its 25 lysines (into arginines) was purchased (Eurofins), and used as template to amplify a DNA fragment with the previous primers. This fragment was then cloned by SLIC technology into *pUASp-attB-HA*.
Transgenesis was performed by Bestgene Inc, at the attP40 site.
pUASp-CHMP1-HA was generated the same way, amplified on pOT2:GH26351 (DGRC) using the primers F: 5'CGCCCGGGGATCAGATCCGCGGCCGCATGTCTACGAGTTCCATGGA3' and R: 5'GGAACATCGTATGGGTACATGGATCCTTCAGCCTGGCGGAGACGTG3'.
pUASp-CHMP2B-HA was generated the same way, amplified on pOT2:LD36173 (DGRC) using the primers F: 5'CGCCCGGGGATCAGATCCGCGGCCGCATGTTCAACAATATTTTCGG3' and R: 5' GGAACATCGTATGGGTACATGGATCCAGAGGAGCGCAGCTTGGCCA3'.
Transgenesis was performed by Bestgene Inc at the attP40 site.

Molecular Biology: constructs for S2 cells transformations

pCasper4-pUbi-attB vector was used, and inserts were cloned by SLIC technology in the vector digested by NotI and BglII.
To produce *pCasper4-pUbi-attB-CHMP1HA*, the insert was amplified on *pUASp-CHMP1-HA* with the following primers: F:
5'GATCCACTAGTGGCCTATGCGGCCGCATGTCTACGAGTTCCATGGA3' and R: 5' ACGTCACCTAGGTGGAGATCTTTAAGCGTAATCTGGAACATC3'.
To produce *pCasper4-pUbi-attB-CHMP2B-HA*, the insert was amplified on *pUASp-CHMP2B-HA* with the following primers: F:
5' GATCCACTAGTGGCCTATGCGGCCGCATGTTCAACAATATTTTCGG3' and R: 5' ACGTCACCTAGGTGGAGATCTTTAAGCGTAATCTGGAACATC3'.
To produce *pCasper4-pUbi-attB-Shrub-HA*, the insert was amplified on *pUASp-Shrub-HA* with the following primers: F:

5’GATCCACTAGTGGCCTATGCGGCCGCATGAGTTTCTTCGGGAAGAT3’ and R: 5’ ACGTCACCTAGGTGGAGATCTTTAAGCGTAATCTGGAACATC3’.

To produce *pCasper4-pUbi-attB-ShrubKR-HA,* the insert was amplified on *pUASp-ShrubKR-HA* with the following primers: F:
5’ CACTAGTGGCCTATGCGGCCGCATGAGTTTCTTCGGGAGGATG3’ and R:
5’ACGTCACCTAGGTGGAGATCTTTAAGCGTAATCTGGAACATC3’.

To generate *pCasper4-pUbi-attB-Shrub-Flag*, a *pCasper4-pUbi-attB-Flag* vector was first constructed by insertion of the Flag tag. Oligonucleotides
5’TCTGATCCCGGGCGGGTACCGACTACAAAGACGATGACGACAAGTAA3’ and
5’CGTCACCTAGGTGGAGATCTTTACTTGTCGTCATCGTCTTTGTAGTC3’ were annealed (complementarity underlined), and inserted by SLIC technology into *pCasper4-pUbi-attB* digested by BglII and KpnI. This Shrub insert was amplified with the following primers: F:
5’GATCCACTAGTGGCCTATGCGGCCGCATGAGTTTCTTCGGGAAGAT3’ and R:
5’ATCGTCTTTGTAGTCGGTACCGTTGGACCAGGATAAAAGCTG3’ and inserted by SLIC technology into *pCasper4-pUbi-attB-Flag* digested by Bgl2 and KpnI.

To generate *pCasper4-pUbi-attB-Usp8-V5* and *pCasper4-pUbi-attB-Usp8-V5*, the inserts were amplified on *pUASp-Usp8-V5* and *pUASp-Usp8-C572A-V5* respectively with the following primers F (for WT and C572A): 5’TCCACTAGTGGCCTATGCGGCCGCATGGCCAAGTTGAAGAAA 3’ and R: 5’CTTACGTCACCTAGGTGGAGATCTTTACGTAGAATCGAGACC 3’ and cloned into *pCasper4-pUbi-attB* digested by BglII and NotI by SLIC technology.

To generate *pCasper4-pUbi-attB-2XHis-Ubiquitin*, the insert was amplified on *pCMV-6XHis-Ubiquitin* (a king gift of G. Legube, Matias Trier) with the primers F:
5’CTAGTGGCCTATGCGGCCGCATGGCTAGCCATCACCATCA3’ and R:
5’CGTCACCTAGGTGGAGATCTTTACCCACCTCTGAGACGGA3’ and cloned by SLIC technology into *pCasper4-pUbi-attB* digested by NotI and AvrII.

Ds-RNA synthesis and treatment

Usp8 dsRNA and control *GFP* dsRNA were synthesized as described in (*18*). Each DNA template for in vitro transcription was prepared using 100ng of cloned cDNA and the following primers :
For *Usp8* : 5’CGAGGAGTACAGACTGGATGG3’and 5’CAGTAGTACGTGAGGTGGGAGG3’ ; For *GFP* : 5’ACGTAAACGGCCACAAGTTC3’ and 5’TGTTCTGCTGGTAGTGGTCG3’. Amplicons were 417bp for *ds-Usp8* and 495bp for *ds-GFP*. Treatment was performed on transfected S2 cells by dsRNA soaking (final concentration 20µg/ml).

Immunostainings on ovaries and testis

Antibody staining and Hoechst staining were performed according to standard protocols. Briefly, ovaries or testis were dissected in PBS, fixed in 4% PFA, rinced and permeabilized in PBT (PBS-0,2%Triton) for 30 min, left overnight with primary antibodies in PBT at 4°C, washed 2 h in PBT, left with secondary antibodies in PBT for 2 hrs at room temperature, washed 1 h in PBT and mounted in Cityfluor. To detect mono or poly-ubiquitinated proteins at the MB of GL cells, ovaries were fixed 10 min in 0.4% PFA, and subsequently treated as mentioned above. The primary antibodies used in this study were the following: mouse-anti-α-spectrin (clone 3A9, DSHB) 1:500; rabbit anti-α-spectrin 1:1000 (*19*), rat-anti-BamC 1:1000 (*8*); rabbit anti-Nanos 1:200 (*20*), rabbit anti-CHMP1 (*21*) 1:200, mouse anti-C3G (a kind gift from Scott Hawley 1A8-1G2) 1:500, rabbit anti-Pav 1:150 (*22*), mouse anti-Ubiquitin clone FK2 (a mix of Enzo Life Sciences, BML-PW8810 and Millipore, 04-263) 1:100 , mouse anti-V5 (Sigma, V8012) 1:100, rabbit anti-HA (Cell signaling technologies C29F4) 1:100, rabbit anti-H3pS10 (Sigma 06-570) 1:1000. Fluorescent secondary antibodies were from Jackson Immunoresearch; Hoechst was from Molecular Probes.

Immunostainings on S2 cells:

Cells were seeded on glass coverslip in 12-well plate (2.10^5 cells/ml) and transfected with 0,4µg DNA using Effectene transfection Reagent (Qiagen). After 72h incubation, cells were fixed in 4% PFA, washed in PBT (PBS-0,1% Triton) and incubated overnight with the following primary antibodies : mouse anti-V5 1:500), rabbit anti-H3pS10 1:1000.

Biochemistry

For western blots of ovary extracts, flies were dissected in PBS, 10 ovaries were homogenized in Laemli 2X and denatured at 95°C. Extracts were loaded on precast Biorad gel (Mini-PROTEAN TGX, #456-9035) and transferred on nitrocellulose membrane (Trans-Blot Turbo Tranfer Pack, #1704158). Membranes were blocked 2 hours in PBS-0,1% Tween-5%BSA and incubated ON at 4°C with mouse anti-V5 antibody (Sigma # V8012) at 1:1000 or anti-tubulin (DM1A, Sigma #T9026) in PBS-0,1% Tween-5%BSA. After 3 washes in PBS -0,1% Tween, the membranes were incubated 2hrs at RT with a peroxydase conjugated anti-mouse IgG (Jackson Immunoresearch #115035174) at 1:10000 in PBS-0,1% Tween-5%BSA. After 3 washes in PBS-0,1% Tween-5%BSA,

bands were detected with the ECL Prime Western Blotting Detection Reagents (GE Healthcare) and visualized using a mini-LAS-4000 Imaging System (Fujifilm).

To **immunoprecipitate HA-tagged ESCRT-III proteins**, pellet of S2 cells were lysed in 1 ml of Lysis Buffer (50 mM Tris pH7.4, 150 mM NaCl, 0.1% NP40, 1 mM EDTA pH8, 10% Glycerol, 1x Complete EDTA-free Protease inhibitor cocktail (Roche) during 30 min at 4°C under rotation at 30 rpm. Homogenates were clarified via two rounds of microfuge centrifugation for 15 min at 4°C. Supernatant was recovered. 50 µl was kept and diluted with 2X Laemli as Input (1/20 of total). The rest of the supernatant was then incubated with 25 µl of pre-washed Pierce™ Anti-HA Magnetic Beads (Thermofisher) under rotation at 15 rpm at RT for 1 hr. Beads were then washed twice with Washing Buffer (WB: 50mM Tris ph7,5; 150mM NaCl; 10% glycerol; 1mM EDTA Ph8; 1x Complete EDTA-free Protease inhibitor cocktail). The pellets were then resuspended in 100 µl of Laemmli 1X-WB 0,5X and denatured at 95 °C for 10 min; bound proteins were recovered from the beads by magnetic separation and analyzed by western blots.

To **immunoprecipitate His-tagged ubiquitinated proteins**, pellets of S2 cells were suspended in 1 ml of TpA (10mM Immidazole; 100mM Na_2HPO4/NaH_2PO4 pH8; Guanidium hydrochloride 6M) and sonicated 3 times 10 sec on ice. After 10 min of centrifugation at 12000 rpm at 4°C. Supernatant was recovered. 50 µl was kept and diluted with 2X Laemli as Input (1/20 of total) .The rest of the supernatent was pre-cleared with 20 µl of A-sepharose beads (Dynabeads Protein A Invitrogen #10001D) for 30 min under rotation at RT. After 10 min centrifugation at 12000 rpm, supernatent was incubated with 50 µl de Ni-NTA-agarose beads (Qiagen, #30210) for 3 hrs under rotation. After 10 min centrifugation at 12000 rpm to pellet the beads, the pellets were washed 3 times in TpA, 3 times in TpB (TpA: TpC 1vol:4vol), 3 times in TpC (Tris –Hcl pH6.8 25mM; Immidazole 20mM) with 1 min centrifugation between each wash. Beads were ultimately eluted in 40 µl of elution buffer (2X SDS loading buffer + β mercapto; 200 mM immidazole), boiled 5 min at 95°C and centrifugated 5 min at 13500 rpm. The supernatents were analyzed by western blot.

Samples (same volume of IP and of Input) were loaded on Biorad precast gels (Mini-PROTEAN TGX, #456-1095), and transfered on nitrocellulose membranes (Biorad Trans-Blot Turbo Tranfer Pack, #1704158). Primary antibodies used after immunoprecipitations were rabbit anti-HA (Sigma, #H6908) 1:1000, mouse anti-V5 (Sigma, #V8012) 1:1000, rabbit anti-Flag (Sigma, #F7425) 1:1000, rabbit anti-USP8 (*7*). Primary antibody dilutions were used several times. Secondary antibodies were from Jackson Immunoresearch. Bands were detected with the ECL Prime Western Blotting Detection Reagents (GE Healthcare) and visualized using a mini-LAS-4000 Imaging System (Fujifilm).

Quantification and Statistics

The number of nuclei per egg chamber was quantified on Hoechst stained ovaries. Quantification of the percentage of egg chambers having more or less than 16 cells were done on one day old females. Chi-square tests were used to compare the proportions of egg chambers having 8, 16 or 32 cells.
Breaking-cyst and stem cyst quantifications were done on germaria immunostained with α-spectrin antibody. Breaking cysts were identified as a group of cells away from the niche whose fusome harbors a narrowing and a bulge in its center. Stem-cysts were identified as a group of cells linked by a fusome, with its anterior most cell being attached to the niche. Chi-square test were used to compare the percentages observed in the different genotypes.
Fluorescence intensity measurements of USP8-GFP and CHMP2B-GFP were done on Z-stack images acquired with identical settings. A Region of Interest (ROI), smaller than a RC width was chosen. For each RC, the mean intensity of three distinct ROIs was quantified by Fiji software. When barely no GFP was detected (in the cyst RCs for CHMP2B-GFP), pav staining was used to position the ROIs on the RCs. Row dataset were transformed into graphics with prism8 software. Chi-square tests were used to compare fluorescence intensity.

Microscopy

Acquisition of Z-stacks on fixed sample was carried out on Zeiss LSM780 or LSM980 confocal microscopes. For live imaging of germarium in figure S1, ovaries were dissected and mounted in oil (10S, Halocarbon, Sigma) and were imaged with an inverted Confocal Spinning Disk Roper/Nikon equipped with a CDD camera CoolSnap HQ2. Time-lapse images were then treated with Fiji.
For the photo-activation experiments, ovaries were dissected and mounted in oil (10S, Halocarbon, Sigma). Photo-activation was done with a 2-photon laser at 820nm (3 iterations, laser power 6%, scan speed = 6; these numbers are rough approximations for the excitation power). Imaging was done with a confocal microscope Zeiss LSM 710.

Supplementary Text

Figure S1 (related to Figure 1)

(A) Fraction of egg chambers exhibiting N nuclei. n represents the number of egg chambers analyzed. Line P{TRiP.HMS01898}attP40 is used as *shRNA-Usp8#1,* and line P{TRiP.HMS01941}attP2 is used as *shRNA-Usp8#2.* (B) Confocal images of fixed ovariole and germarium of females expressing *shRNA-Usp8#1* under the control of *nos-GAL4* driver. Scale bar: 20 μm in B, 10 μm in B'. B" is a close-up view of the cyst framed in B'. Dotted lines surround a breaking 8CC. The ectopic MB is indicated by a white arrow. (C) Fraction of germaria with at least one breaking cyst. Line P{TRiP.HMS01898}attP40 is used as *shRNA-Usp8#1*. n represents the number of germarium analyzed. (D-E) Selected time points of live imaging experiments performed on germaria expressing *Par1-GFP* (to visualize the fusome) and *Tubulin-PA-GFP* and *shRNA-Usp8#2* (P{TRiP.HMS01941}attP2) (D) or *Par1-GFP* and *Tubulin-PA-GFP* only (E) under the *nos-GAL4* promoter. Tub-PA-GFP is photoactivated (PA) in the region defined by the red circle, and the fluorescence diffusion to the neighboring cells is observed. D-Top: in a 2-cell cyst (2CC), whose fusome does not exhibit a MB, Tub-GFP proteins diffuse from the activated cell into the other. D-Middle: when activated in a GSC that has a MB, Tub-GFP do not diffuse from the GSC to the CB. D-Bottom: when activated in one cell of a 2CC that has a MB, Tub-GFP do not diffuse to the sister cell. Cytoplasmic isolation is achieved when the MB is visible. E: when activated in a WT 4CC, Tub-GFP diffuse in the whole cyst. Scale bar: 10 μm. On the right, schematic representation of the Tubulin-PA-GFP diffusion, where Tub-PA-GFP is in green and the fusome (Par-1-GFP) is in red. (F-G) Confocal image of live-imaged germaria from a female expressing *shRNA-Usp8* (P{TRiP.HMS01941}attP2) and *Par1-GFP* (G) or *Par1-GFP* alone (F) to follow the breaking of the fusome of a GSC/CB pair in WT (F) or of a breaking 2CC (G). On the right, are close up extracted from the movies. Time (min) are indicated. The white arrows point to the MBs. F: The MB is cut between 18 and 20 min, the fusome remaining in the GSC retracts to the anterior, and the MB.remains on the CB. G: The MB is cut between 20 min and 21 min and gets inherited by one of the two single cell (the bottom one). As Par-1-GFP fades, the top cell enters mitosis at 51 min, while the bottom one remains in interphase for at least 20 more minutes . Scale bar: 10 μm (H-I) Confocal images of the anterior tip of the testis of males expressing *shRNA-white* (H) or *shRNA-Usp8#2* (I, P{TRiP.HMS01941}attP2) under the control of *nos-GAL4* driver. H' and I' are close-up views of the 4CC framed in H and I. Dotted lines surrounds cysts, the white arrow indicates the MB of the breaking cyst. Scale bar: 10 μm. (J) Confocal image of an ovariole from a female with $Usp8^{KO}$ GLC (RFP negative cells). Three mutant egg chambers are

formed of only 4 nuclei. (K) Fraction of *Usp8^{KO}* mutant egg chambers made of 4, 8 or 16 cells. n represent the total number of GLC clones analyzed (4 experiments). (L) Confocal image of a germarium from a female with *Usp8^{KO}* GLC (RFP negative cells). An internal control, RFP positive, non-breaking cyst is outlined with a red dotted line, and a mutant, RFP negative, breaking cyst is outlined with a white dotted line. None of them expresses Nanos. Scale bar: 10 μm. (M-N) Confocal images of fixed germaria of females expressing *shRNA-white* (M) or *shRNA-Usp8* (N, P{TRiP.HMS01941}attP2) under the control of *nos-GAL4* driver. Scale bar: 10 μm. (O) Confocal image of an egg chamber from a female expressing *Usp8-WT* under the control of the somatic *traffic-jam-GAL4* driver, stained with α-H3pS10 (PH3) antibody to detect mitotic cells. Two perfectly synchronous clusters in metaphase are surrounded by dotted lines. Scale bar: 10 μm. (P) Fraction of mitotic follicular cells found in synchronous cluster on the Y axis. Genotypes are on the X axis. *alix^{1}* mutants were reported to have abscission delay in GSC; here we show that they also exhibit an abscission delay in the somatic follicular epithelium, similar to the one induced by overexpression of USP8-WT. n represents the number of mitotic cells. P values are derived from Chi Square test. Ns: non significant. (Q-T) Confocal images of S2 cells expressing Usp8-WT-V5 stained with α-H3pS10 (PH3) antibody to detect mitotic cells and α-V5 to detect USP8-V5. Metaphase cells (Q-R) were mostly single cells, but could also be still linked by a MB (white arrow in R) to a sister cell. PH3 negative cells with a MB stained for USP8-V5 (S-T) were mostly late cytokinesis cells (S), but could also be found in a cluster of 4 cells (T). Both R and T indicate delayed abscission events. Scale bar: 5 μm (U) Fraction of S2 cells with the cluster phenotype as shown in R and T among figures as in (Q-T). (U) Fraction of S2 cells found in cluster as in R and T over the total number of S2 cells as in (Q-T). n represents the number of cells. P values (bold) are derived from Chi Square test.

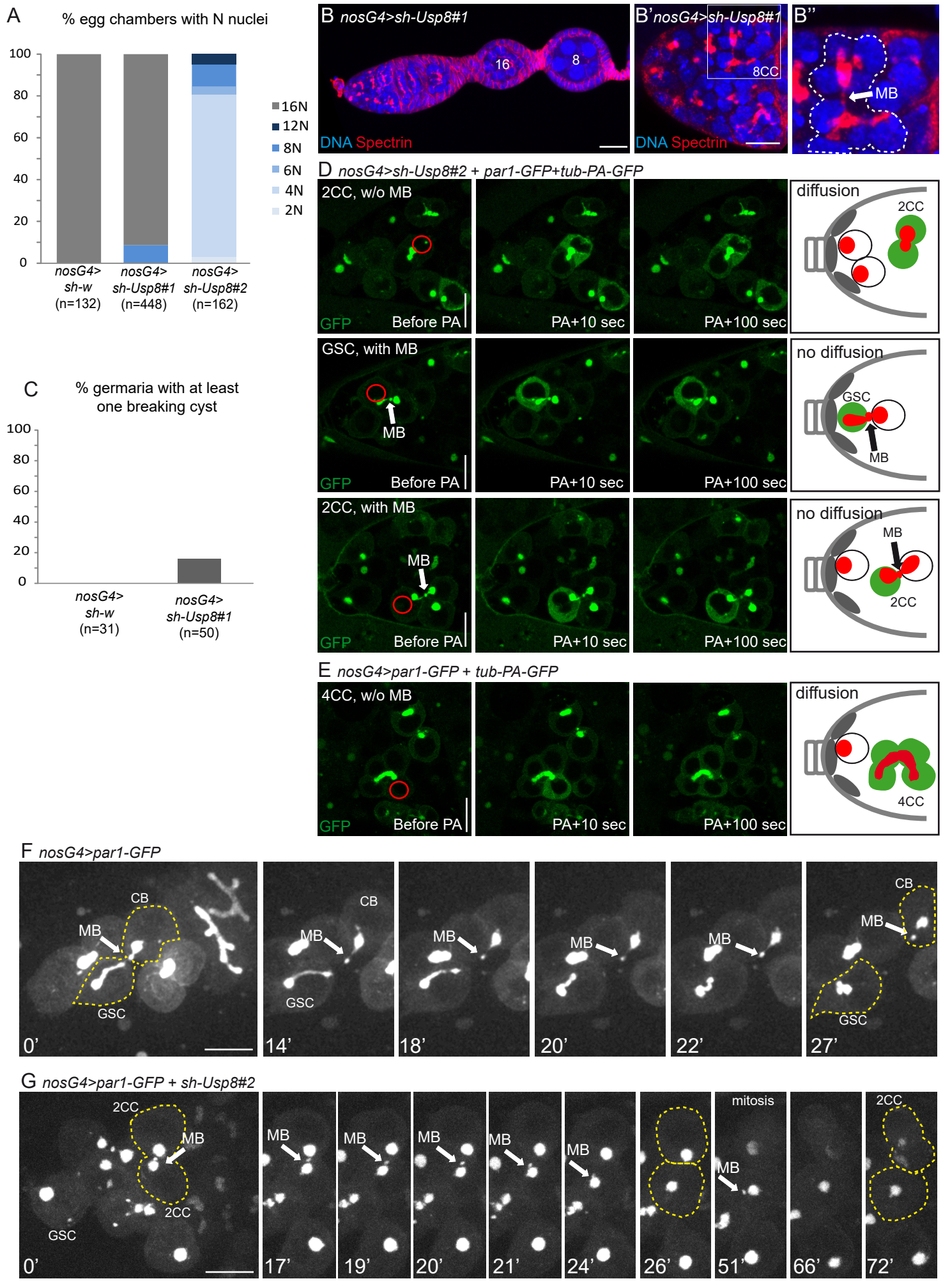

Figure S1 page 1

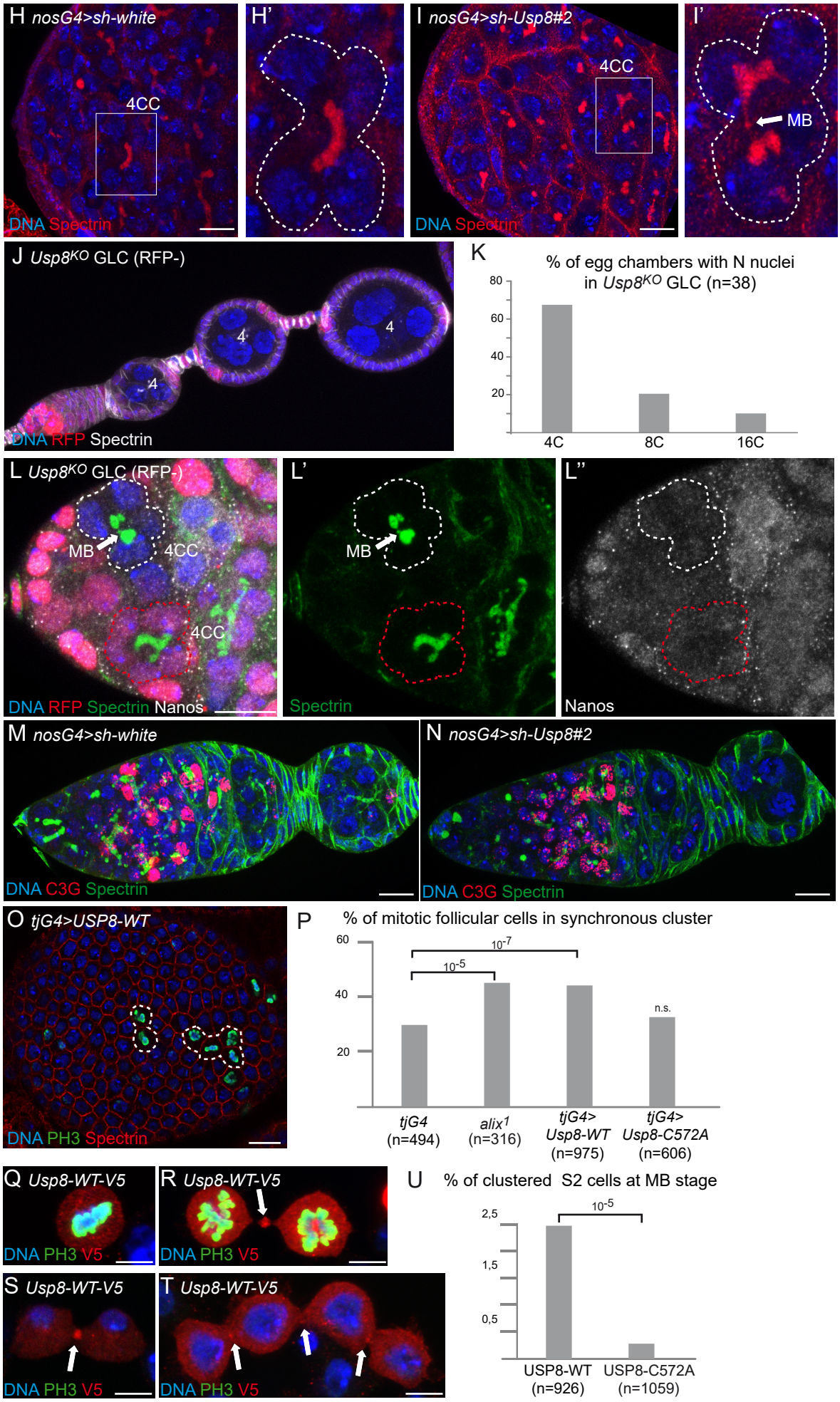

Figure S1 page 2

Figure S2 (related to Figure 2)

(A) Confocal image of a germarium from a female with *Usp8^{KI}* GLC (RFP negative cells). Dotted lines surround a non-breaking germline cyst. Breaking cysts were never observed in such GLC (n=15) indicating that the USP8-GFP product from the *Usp8^{KI}* locus is functional to block abscission. (B) Immunoblots of ovary extracts from females expressing *Usp8* variants under the control of *nos-GAL4* driver. Genotypes are on top. Membranes were blotted for V5 (USP8-V5) and Tubulin. USP8-C572A is expressed at the same level than USP8-WT. Immunoblot representative of 2 experiments. (C-E) Confocal images of germaria from females with *Usp8^{KO}* GLC (RFP negative cells) expressing either *Usp8-WT-V5* (C), or *Usp8-C572A-V5* (D) or no transgene (B) under the control of *bam-GAL4* driver and stained for Ubiquitin (Ubi) and α-Spectrin. Dotted lines surround mutant cysts. White arrows indicate ectopic MBs observed in mutant (C) and non rescued (E) cysts, but not in the rescued (D) one. Ubiquitin aggregates are found in the cytoplasms of mutant (C) and non rescued (E) *Usp8* GLC. Scale bar: 10 μm. (F) Confocal images of a germarium from a female with a *Usp8^{KO}* GLC (GFP negative cells) expressing *Usp8-C572A-V5* under the control of *bam-GAL4* driver and stained with α-Ubiquitin (Ubi) and α-V5. F',F" and F"' are close up of the 4CC framed in F. USP8-C572A-V5 forms cytoplasmic aggregates that are co-stained with Ubi and probably correspond to enlarged endosomes (EE, yellow arrows, see G and H). The white arrow indicates the MB of the non-rescued cyst. USP8-C572A-V5 expressing non-mutant cyst also exhibit cytoplasmic aggregates costained with Ubi. Scale bar: 10 μm. (G-H) Confocal images of germaria from females expressing either Rab5-YFP (G) or Rab7-YFP (H) and *Usp8-C572A-V5* under the control of *bam-GAL4* driver and stained with α-Ubiquitin (Ubi) and α-V5. The cytoplasmic USP8-C572A-V5 aggregates co-localize with both endosomal markers, indicating that they are enlarged endosomes (EE, yellow arrows).The central RC (red arrows) are devoid of Rab5-YFP and Rab7-YFP. The expression of USP8-C572A-V5 is not sufficient to induce ectopic abscission in these WT cysts, so it does not behave as a dominant negative version of USP8 for abscission. G', G" and G"' are close up views of the 8CC framed in G; H', H" and H"' are close up views of the 8CC framed in H. Scale bar: 10 μm. (I) Confocal images of the anterior tip of the testis of a male expressing GFP tagged *Usp8* from the endogenous locus. I' and I" are close-up view of a 4CC (top) and a GSC/GB pair (bottom) framed in I. The white arrow indicates the MB between the GSC and the GB, the red arrows indicate the RC in the 4-cell cyst. Scale bar: 10 μm. (J) Confocal images of somatic follicular cells expressing GFP tagged *Usp8* from the endogenous locus stained

for α-Spectrin. J’ and J” show separate channels. USP8-GFP is detected in a gap of α-Spectrin between two synchronous mitotic follicular cells, at a RC (red arrow). Scale bar: 5 μm.

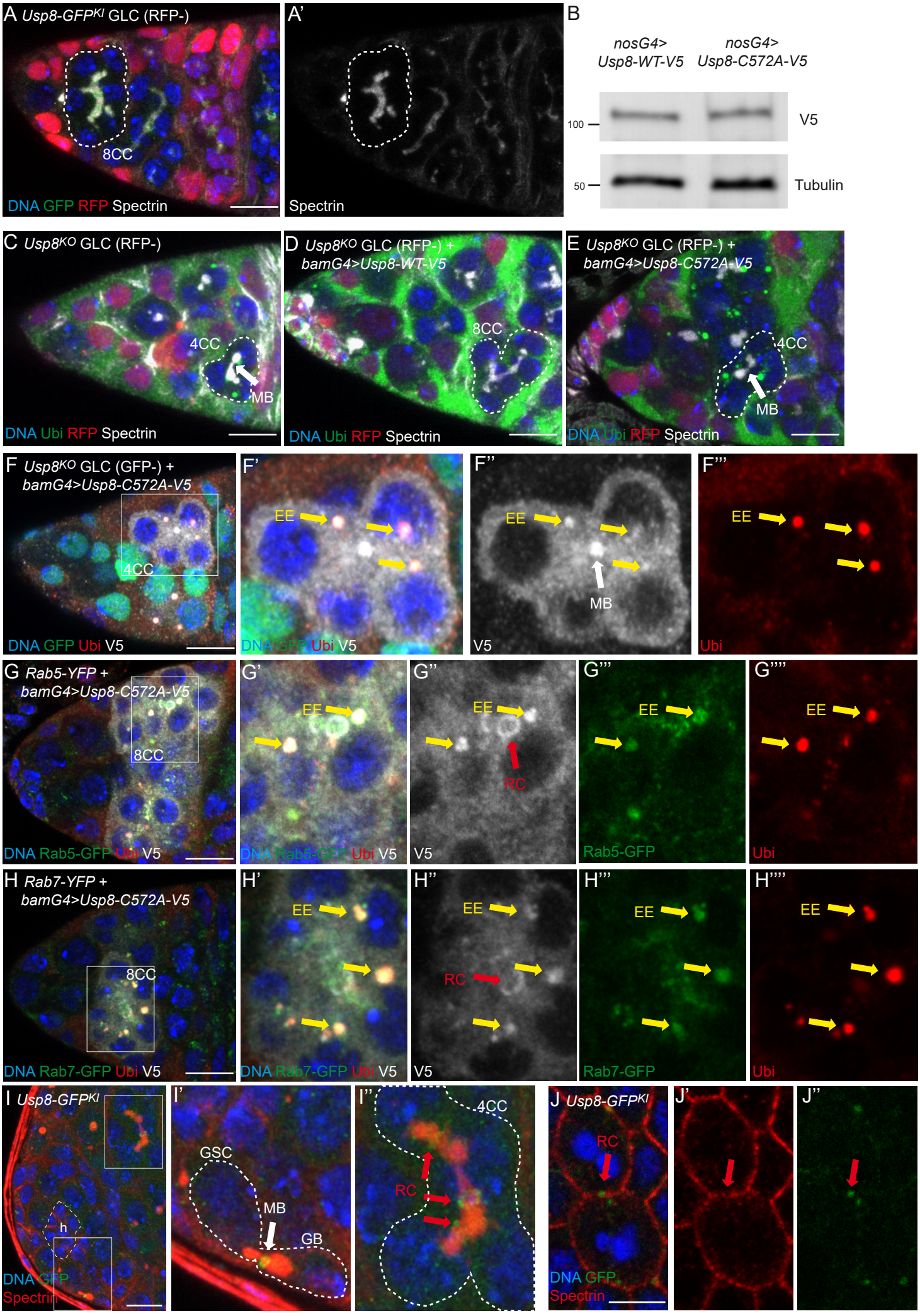
A Usp8-GFPKI GLC (RFP-)
8CC
DNA GFP RFP Spectrin
A'
Spectrin
B
nosG4> Usp8-WT-V5
nosG4> Usp8-C572A-V5
100
V5
50
Tubulin
C Usp8KO GLC (RFP-)
4CC
MB
DNA Ubi RFP Spectrin
D Usp8KO GLC (RFP-) + bamG4>Usp8-WT-V5
8CC
DNA Ubi RFP Spectrin
E Usp8KO GLC (RFP-) + bamG4>Usp8-C572A-V5
4CC
MB
DNA Ubi RFP Spectrin
F Usp8KO GLC (GFP-) + bamG4>Usp8-C572A-V5
4CC
DNA GFP Ubi V5
F'
EE
DNA GFP Ubi V5
F''
EE
MB
V5
F'''
EE
Ubi
G Rab5-YFP + bamG4>Usp8-C572A-V5
8CC
DNA Rab5-GFP Ubi V5
G'
EE
DNA Rab5-GFP Ubi V5
G''
EE
RC
V5
G'''
EE
Rab5-GFP
G''''
EE
Ubi
H Rab7-YFP + bamG4>Usp8-C572A-V5
8CC
DNA Rab7-GFP Ubi V5
H'
EE
DNA Rab7-GFP Ubi V5
H''
EE
RC
V5
H'''
EE
Rab7-GFP
H''''
EE
Ubi
I Usp8-GFPKI
h
DNA GFP Spectrin
I'
GSC
MB
GB
I''
4CC
RC
J Usp8-GFPKI
RC
DNA GFP Spectrin
J'
J''

Figure S2

Figure S3 (related to Figure 3)

(A) Immunoblots of Input (In, 1/20 of the IP) or Immunoprecipitated (IP) ESCRT-III proteins from S2 cells expressing ESCRT-HA and V5-tagged USP8 variants. Membranes were blotted with α-HA antibody. Three ESCRT-III were tested. Arrows indicate HA-tagged ESCRT-III. (B) Immunoblots of Input (In, 1/20 of the IP) or Immunoprecipitated (IP) ubiquitinated proteins from S2 cells expressing ESCRT-HA, His-tagged Ubiquitin, and V5-tagged USP8 variants. Membrane were blotted with α-V5 antibody. Arrows indicate V5-tagged USP8. (C-D) Immunoblots of Input (In, 1/10 of the IP) or Immunoprecipitated (IP) ubiquitinated proteins from S2 cells transfected with *Ubi-His* and *Shrub-HA* (C) or *CHMP2B-HA* (D) and treated with double-strand RNA directed against *GFP* (*ds-GFP*) or *Usp8* (*ds-Usp8*). Membranes were blotted with α-HA antibody. Arrows indicate HA-tagged ESCRT-III. *ds-Usp8* induces an increase in ubiquitinated Shrub and CHMP2B levels. Blots are representative of 3 experiments. (E) Immunoblot of lysate of S2 cells treated with double-strand RNA directed against *GFP* (*ds-GFP*) or *Usp8* (*ds-Usp8*). Membrane was blotted with α-USP8. *ds-Usp8* is efficient in reducing USP8 levels. This blot is representative of 3 experiments. (F-G) Confocal images of germaria from *Shrb-GFP*^{KI} females expressing (G) or not (F) *shRNA-Usp8* (P{TRiP.HMS01941}attP2) under the control of *nos-GAL4* driver. F' and F" are close up views of the regions framed in F. G' is a close-up view of the region framed in G. In F', the white dotted line surrounds a GSC/CB pair, whose RC is Shrub-GFP positive, in F", the yellow dotted line surrounds a 4CC, whose RC are Shrub-GFP negative. In G', the dotted line surrounds a breaking 4CC. White arrow indicates the ectopic MB marked by Shrub-GFP, and red arrows indicate Shrub-GFP positive RCs. Scale bar: 10 μm. (H-I) Confocal images of germaria from females expressing CHMP2B-GFP. H' and I' are close-up views of the regions framed in H and I. Dotted line surrounds a GSC/CB pair (H') whose MB (white arrow) is CHMP2B-GFP positive, and a 8CC (I') whose RC are CHMP2B-GFP negative. Scale bar: 10 μm. (J) Confocal image of a germaria from a CHMP2B-GFP expressing female with a *Usp8*^{KO} GLC. J' is a close up view of the 4-cell cyst framed in J. The dotted line surrounds the breaking 4CC, whose MB (white arrow) and RCs (red arrows) are CHMP2B-GFP positive. Scale bar: 10 μm. (K-L) Confocal images of germaria from *white* females immunostained for α-Spectrin and CHMP1. K' and L' are close up views of the regions framed in K and L. In K', the white dotted line surrounds a GSC/CB pair, whose RC (red arrow) is CHMP1 positive, in L', the dotted line surrounds a 4CC, whose RC are not CHMP1 positive. Scale bar: 10 μm. (M) Confocal images of a germarium from a female with *Usp8*^{KO} GLC (RFP negative cells) immunostained for Spectrin and CHMP1. M', M" and M"' are close up of the mutant 8CC framed in M. CHMP1 is

ectopically localized at the MB (white arrow) and RCs (red arrows). (N-O) Confocal images of testis from males expressing *Shrub-HA* alone (N) or together with *sh-Usp8* (O, P{TRiP.HMS01941}attP2) stained for HA and α-Spectrin. N' and N" are close up views of the GSC/GB pair (N') or of the 8CC (N") framed in F. Shrub-HA is detected at the RC (red arrow) between the GSC and the gonioblast (GB), but not in the cyst. O' is a close up view of several 2-cell cysts framed in O. The dotted line in O' surrounds a breaking 2CC whose MB (white arrow) is positive for Shrub-HA. A RC (red arrow) is also Shrub-HA positive in a neighboring 2-cell cyst. Scale bar: 10 μm. h is the surrounded hub. (P-Q) Confocal images of testis from males expressing *CHMP2B-GFP* together with *sh-white* (P) or *sh-Usp8* (Q, P{TRiP.HMS01941}attP2) stained for α-spectrin. P' and P" are close up views of the GSC/GB pair (P') or of the 2CC (P") framed in P. CHMP2B-GFP is detected at the MB (white arrow) between the GSC and the gonioblast (GB), but not in the cyst. Q' is a close up of a breaking 4CC and of a 2CC framed in Q. The dotted line in Q' surrounds a breaking 4CC whose MB (white arrow) is CHMP2B-GFP positive. A RC (red arrow) is also CHMP2B-GFP positive in a neighboring 2-cell cyst. h is the surrounded hub. Scale bar: 10 μm. (R) Fraction of egg chambers exhibiting N nuclei. n represent the numbers of egg chambers analyzed. (S) Fraction of 4CC exhibiting a breaking phenotype. P value (p) is derived from Chi Square test. n represent the numbers of cysts analyzed (T) Fraction of egg chambers exhibiting N nuclei. n represent the numbers of egg chambers analyzed.

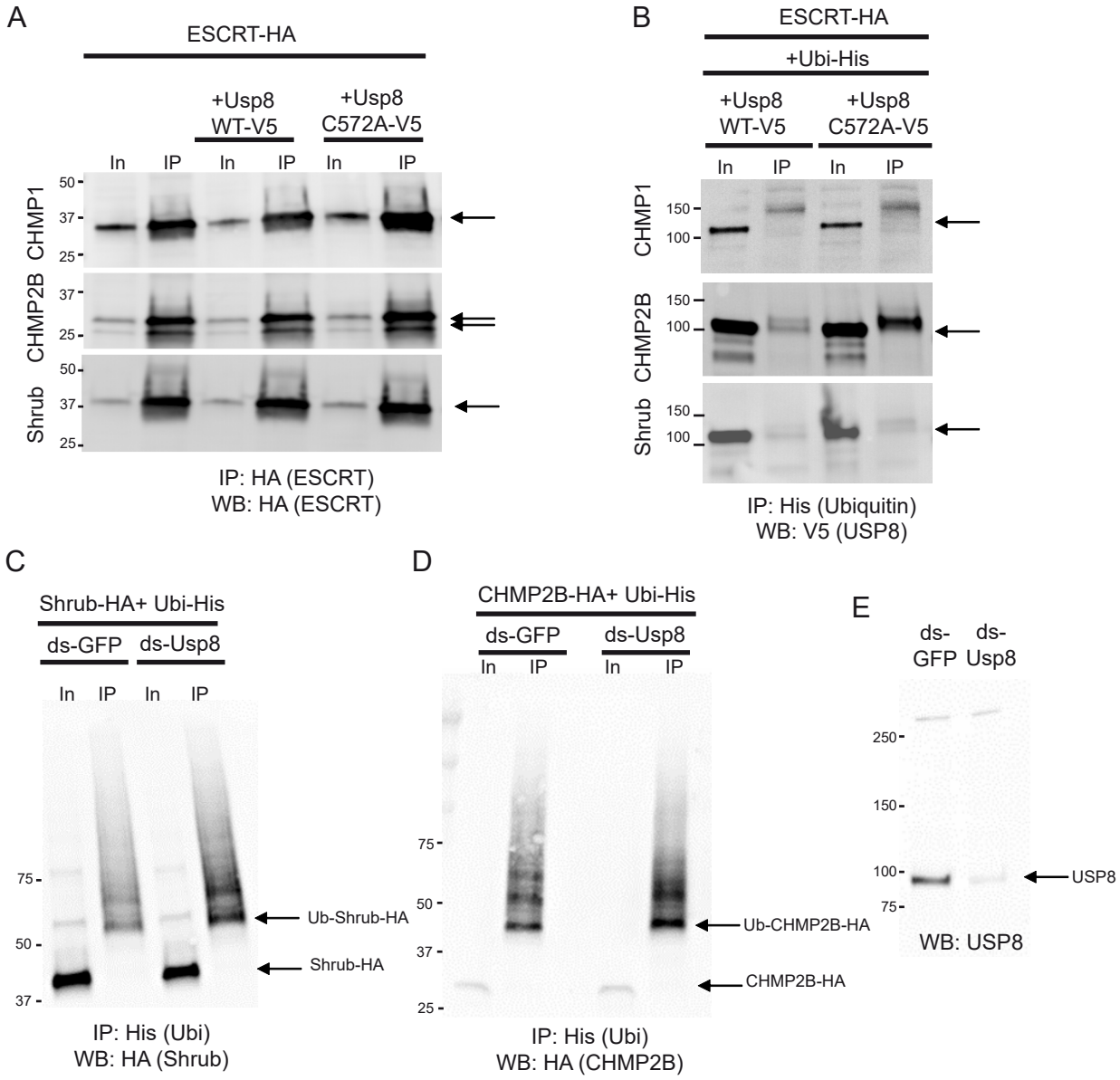

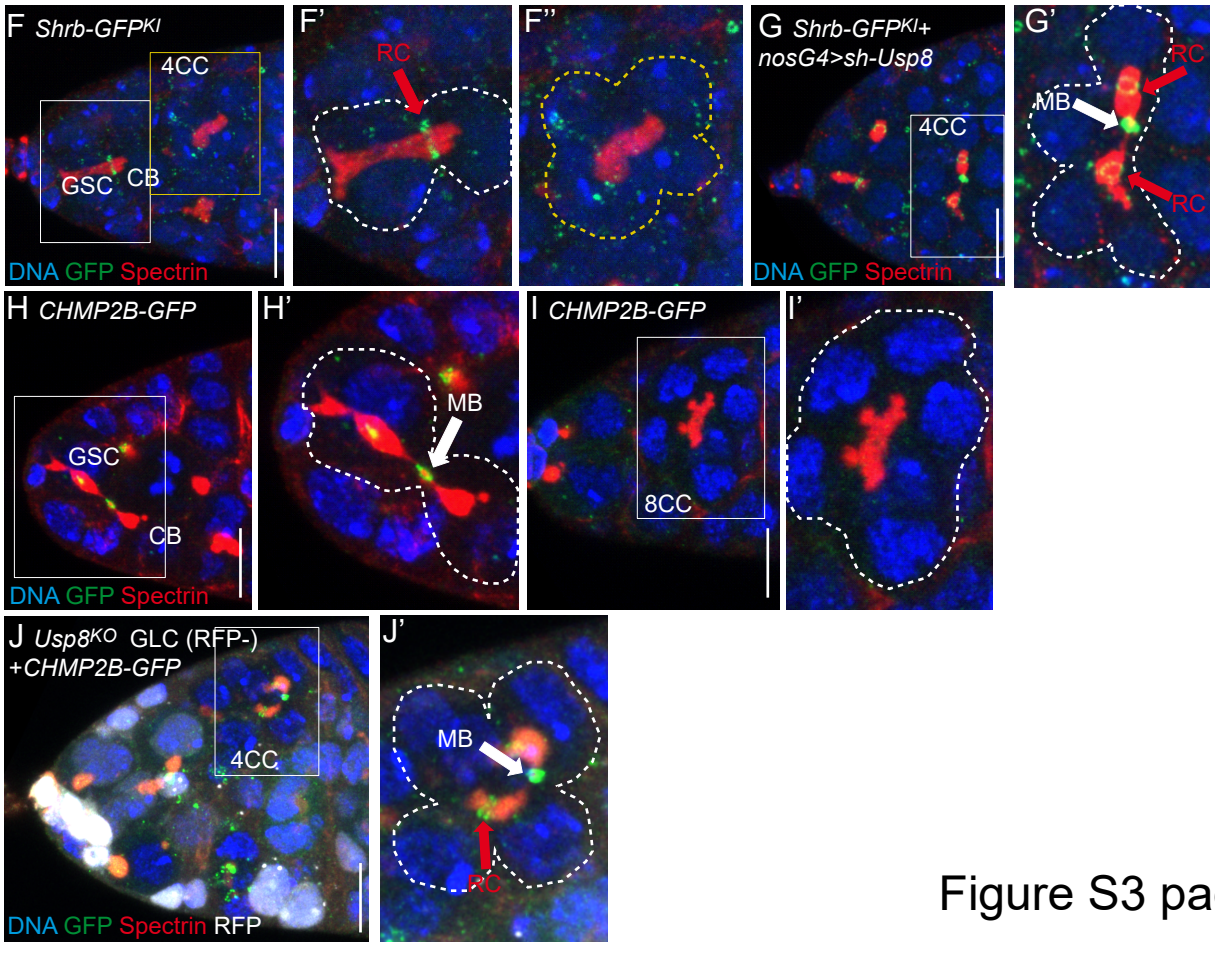

Figure S3 page 1

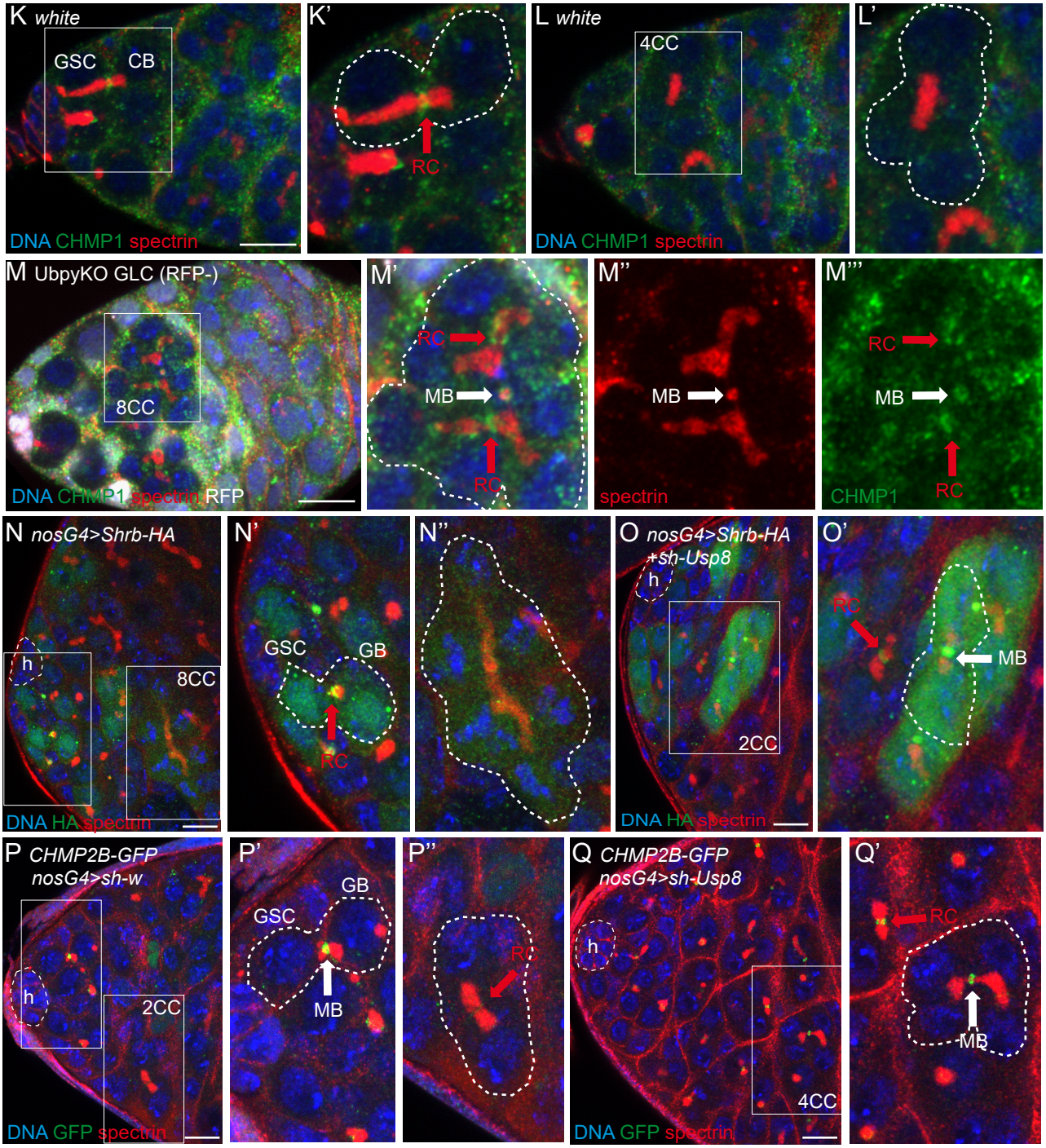

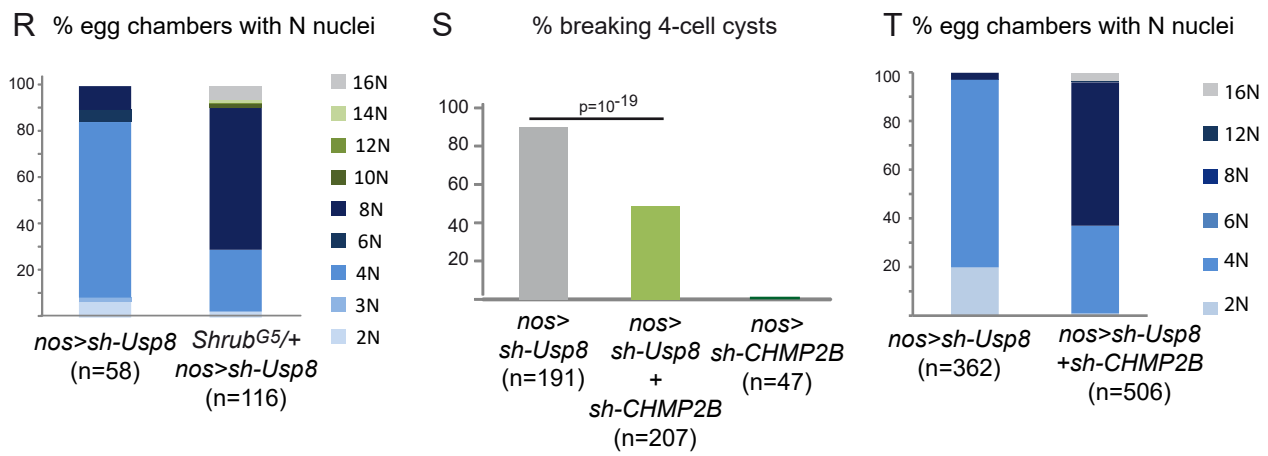

Figure S3 page 2

Figure S4 (related to figure 4)

(A) Scheme of Shrub protein sequence. Blue arrows indicate the position of the 25 lysines that were mutated into arginines. (B) Immunoblots of Input (In, 1/20 of total extract) or Immunoprecipitated (IP) ubiquitinated proteins from S2 cells transfected with *Shrub-WT-HA* or *Shrub-KR-HA* and *Ubi-His* or an empty vector (-). Membrane was blotted with HA antibody. Shrub-WT is ubiquitinated in S2 cells while Shrub KR is not. Immunoblot representative of 2 experiments. (C) Confocal image of a germaria of a $shrb^{G5}$ /+ female expressing *Shrb-WT-HA* under the control of *nos-GAL4* driver. The dotted line surrounds a GSC/CB pair. The red arrow indicates the RC positive for Shrb-WT-HA. Scale bar:10 μm. (D) Immunoblot of Input (In, 1/20 of total extract) or Immunoprecipitated (IP) HA tagged proteins from S2 cells transfected with *Shrub-WT-HA* or *Shrub-KR-HA* and *Shrub-Flag*. Membrane was blotted with Flag antibody. Both Shrub-WT and Shrub-KR bind Shrub-Flag. NS: non-specific band. Immunoblot representative of 2 experiments. (E) Confocal images of a germaria with $shrb^{G5}$ GLC from a female expressing *Shrb-KR-HA* under the control of *nos-GAL4* driver. The dotted line surrounds a GSC/CB pair. The red arrow indicates a very faint Shrb-KR-HA staining detected on the RC. Such weak staining was observed in 1 of the 6 rescued $shrb^{G5}$ GLC, and in 3 of the 24 non rescued $shrb^{G5}$ GLC . Scale bar:10 μm.

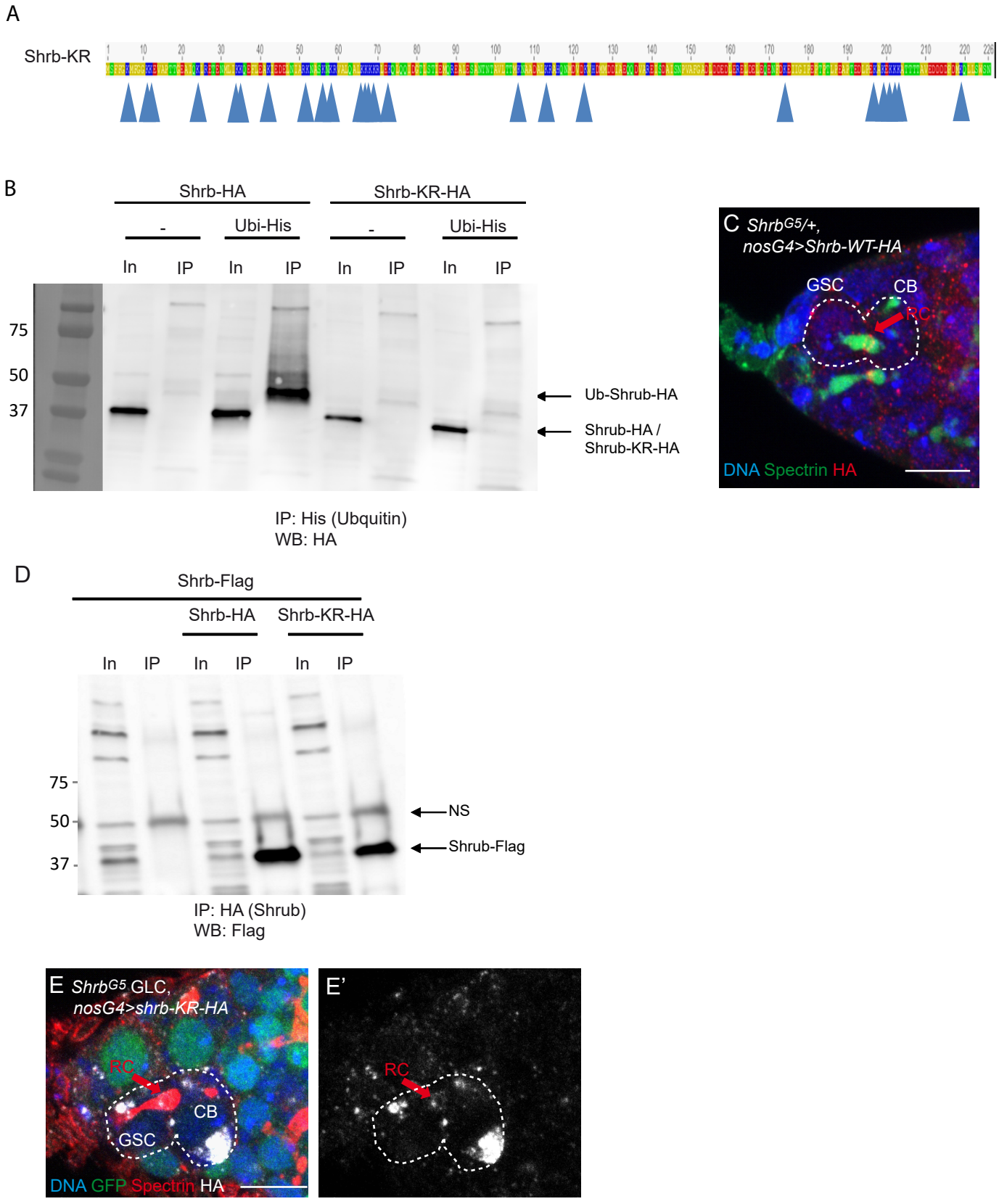
A
Shrb-KR
B
Shrb-HA
Shrb-KR-HA
-
Ubi-His
-
Ubi-His
In
IP
In
IP
In
IP
In
IP
75
50
37
Ub-Shrub-HA
Shrub-HA /
Shrub-KR-HA
IP: His (Ubquitin)
WB: HA
C
ShrbG5/+,
nosG4>Shrb-WT-HA
GSC
CB
RC
DNA Spectrin HA
D
Shrb-Flag
Shrb-HA
Shrb-KR-HA
In
IP
In
IP
In
IP
75
50
37
NS
Shrub-Flag
IP: HA (Shrub)
WB: Flag
E
ShrbG5 GLC,
nosG4>shrb-KR-HA
RC
CB
GSC
DNA GFP Spectrin HA
E'
RC

Figure S4

Movie 1 (Related to Figure S1D)

Live imaging experiment performed on a germarium expressing *shRNA-Usp8* (P{TRiP.HMS01941}attP2), *Par1-GFP* (to visualize the fusome) and *Tubulin-PA-GFP* under the *nos-GAL4* promoter. Tub-PA-GFP is photoactivated (PA) in the region defined by the red circle, and the fluorescence diffusion to the neighboring cells is observed. Images are acquired every 10 sec after PA.In a 2-cell cyst (2CC), whose fusome does not exhibit a MB, the Tub-PA-GFP diffuses from the activated cell into the other cell of the cyst.

Movie 2 (Related to Figure S1D)

Live imaging experiment performed on a germarium expressing *shRNA-Usp8* (P{TRiP.HMS01941}attP2), *Par1-GFP* (to visualize the fusome) and *Tubulin-PA-GFP* under the *nos-GAL4* promoter. Tub-PA-GFP is photoactivated (PA) in the region defined by the red circle, and the fluorescence diffusion to the neighboring cells is observed. Images are acquired every 10 sec after PA. Here, tub-PA-GFP is activated in a GSC that has a MB, it does not diffuse from the GSC to the CB.

Movie 3 (Related to Figure S1D)

Live imaging experiment performed on a germarium expressing *shRNA-Usp8* (P{TRiP.HMS01941}attP2), *Par1-GFP* (to visualize the fusome) and *Tubulin-PA-GFP* under the *nos-GAL4* promoter. Tub-PA-GFP is photoactivated (PA) in the region defined by the red circle, and the fluorescence diffusion to the neighboring cells is observed. Images are acquired every 10 sec after PA. Here, tub-PA-GFP is activated in a 2-cell cyst (2CC) that has a MB, tub-GFP does not diffuse to the sister cell.

Movie 4 (Related to Figure S1E)

Live imaging experiment performed on a germarium expressing *Par1-GFP* (to visualize the fusome) and *Tubulin-PA-GFP* under the *nos-GAL4* promoter. Tub-PA-GFP is photoactivated (PA) in the region defined by the red circle in one cell of a 4CC, and the fluorescence diffusion to the neighboring cells is observed. Images are acquired every 10 sec after PA. Here, tub-GFP diffuses to all the three sister cell.

Movie 5 (related to Figure S1F)

Germarium imaged live from a female expressing and *Par1-GFP* under the *nos-GAL4* promoter to follow the breaking of the fusome between the GSC and its daughter CB. Images are acquired every 1 min. The MB is indicated by a red arrow at tp0.

Movie 6 (related to Figure S1G)

Germarium imaged live from a female expressing *shRNA-Usp8* (P{TRiP.HMS01941}attP2) and *Par1-GFP* under the *nos-GAL4* promoter to follow the breaking of the fusome of a 2-cell cyst. Images are acquired every 1 min. The MB is indicated by a red arrow at tp0.

References

1. M. Van Doren, A. L. Williamson, R. Lehmann, Regulation of zygotic gene expression in Drosophila primordial germ cells. *Curr Biol* **8**, 243-246 (1998).
2. M. Clemot, A. Molla-Herman, J. Mathieu, J. R. Huynh, N. Dostatni, The replicative histone chaperone CAF1 is essential for the maintenance of identity and genome integrity in adult stem cells. *Development* **145**, (2018).
3. D. Chen, D. M. McKearin, A discrete transcriptional silencer in the bam gene determines asymmetric division of the Drosophila germline stem cell. *Development* **130**, 1159-1170 (2003).
4. T. Vaccari *et al.*, Comparative analysis of ESCRT-I, ESCRT-II and ESCRT-III function in Drosophila by efficient isolation of ESCRT mutants. *J Cell Sci* **122**, 2413-2423 (2009).
5. M. J. Murray, R. Saint, Photoactivatable GFP resolves Drosophila mesoderm migration behaviour. *Development* **134**, 3975-3983 (2007).
6. J. R. Huynh, J. M. Shulman, R. Benton, D. St Johnston, PAR-1 is required for the maintenance of oocyte fate in Drosophila. *Development* **128**, 1201-1209 (2001).
7. A. Mukai *et al.*, Balanced ubiquitylation and deubiquitylation of Frizzled regulate cellular responsiveness to Wg/Wnt. *EMBO J* **29**, 2114-2125 (2010).
8. D. McKearin, B. Ohlstein, A role for the Drosophila bag-of-marbles protein in the differentiation of cystoblasts from germline stem cells. *Development* **121**, 2937-2947 (1995).
9. B. Ohlstein, D. McKearin, Ectopic expression of the Drosophila Bam protein eliminates oogenic germline stem cells. *Development* **124**, 3651*3662 (1997).
10. A. H. Eikenes *et al.*, ALIX and ESCRT-III coordinately control cytokinetic abscission during germline stem cell division in vivo. *PLoS Genet* **11**, e1004904 (2015).
11. M. Sarov *et al.*, A genome-wide resource for the analysis of protein localisation in Drosophila. *Elife* **5**, e12068 (2016).
12. R. Pancratov *et al.*, The miR-310/13 cluster antagonizes beta-catenin function in the regulation of germ and somatic cell differentiation in the Drosophila testis. *Development* **140**, 2904-2916 (2013).
13. G. Bodon *et al.*, Charged multivesicular body protein 2B (CHMP2B) of the endosomal sorting complex required for transport-III (ESCRT-III) polymerizes into helical structures deforming the plasma membrane. *J Biol Chem* **286**, 40276-40286 (2011).
14. A. H. Brand, N. Perrimon, Targeted gene expression as a means of altering cell fates and generating dominant phenotypes. *Development* **118**, 401-415 (1993).
15. T. B. Chou, N. Perrimon, Use of a yeast site-specific recombinase to produce female germline chimeras in Drosophila. *Genetics* **131**, 643-653 (1992).
16. T. Xu, G. M. Rubin, Analysis of genetic mosaics in developing and adult Drosophila tissues. *Development* **117**, 1223-1237 (1993).
17. D. Pinheiro *et al.*, Transmission of cytokinesis forces via E-cadherin dilution and actomyosin flows. *Nature* **545**, 103-107 (2017).
18. C. Li, P. D. Zamore, RNAi in Mammalian Cells by siRNA Duplex Transfection. *Cold Spring Harb Protoc* **2019**, (2019).
19. T. J. Byers, R. Dubreuil, D. Branton, D. P. Kiehart, L. S. Goldstein, Drosophila spectrin. II. Conserved features of the alpha-subunit are revealed by analysis of cDNA clones and fusion proteins. *J Cell Biol* **105**, 2103-2110 (1987).

20. K. Hanyu-Nakamura, S. Kobayashi, A. Nakamura, Germ cell-autonomous Wunen2 is required for germline development in Drosophila embryos. *Development* **131**, 4545-4553 (2004).
21. T. Matusek *et al.*, The ESCRT machinery regulates the secretion and long-range activity of Hedgehog. *Nature* **516**, 99-103 (2014).
22. R. R. Adams, A. A. M. Tavares, A. Salzberg, H. J. Bellen, D. M. Glover, pavarotti encodes a kinesin-like protein required to organize the central spindle and contractile ring for cytokinesis. *Genes Dev* **12**, 1483-1494 (1998).

Table of genotypes

Figure 1

(C, D) *w*;; nos-Gal4/UAS-shRNA-w* (P{TRiP.GL00094}attP2)

(E, F) *w*;; nos-Gal4*/*UAS-shRNA-Usp8* (P{TRiP.HMS01941}attP2)

(G) same as (C) and (E)

(H, I) *hs-FLP/+;bam-bam-GFP/+; FRT82, Usp8^{KO}/FRT82, Ubi-nls-RFP*

(J, K) *UAS-Ubpy-WT-HA/+; nos-Gal4/+*

(M) *UAS-Ubpy-C572A-HA/+; nos-Gal4/+*

(L) *UAS-Ubpy-WT-HA/+; nos-Gal4/+*

UAS-GFP/nos-Gal4

UAS-Ubpy-C572A-HA/+; nos-Gal4/+

Figure 2

(B) *hs-FLP/+;; FRT82, Usp8^{KO}/FRT82, Ubi-nls-RFP*

hs-FLP/+;bam-Gal4, UAS-Usp8-WT-V5/+; FRT82, Usp8^{KO}/FRT82, Ubi-nls-RFP

hs-FLP/+;bam-Gal4, UAS-Usp8-C572A-V5/+; FRT82, Usp8^{KO}/FRT82, Ubi-nls-RFP

(C) *hs-FLP/+;; FRT82, Usp8^{KO}/FRT82, Ubi-nls-RFP*

(D) *hs-FLP/+;bam-Gal4, UAS-Usp8-WT-V5/+; FRT82, Usp8^{KO}/FRT82, Ubi-nls-RFP*

(E) *hs-FLP/+;bam-Gal4, UAS-Usp8-C572A-V5/+; FRT82, Usp8^{KO}/FRT82, Ubi-nls-RFP*

(F) *w*;; nos-Gal4/UAS-shRNA-w* (P{TRiP.GL00094}attP2)

(G) *w*;; nos-Gal4*/*UAS-shRNA-Usp8* (P{TRiP.HMS01941}attP2)

(H-I) *w*;; Usp8^{KI}/+*

Figure 3

(C,D) *nos-Gal4, UAS-Shrub-HA/+*

(E) *hs-FLP/+; nos-Gal4, UAS-Shrub-HA/+; FRT82, Usp8^{KO}/FRT82, Ubi-nls-RFP*

(F, I) *w*; nos-Gal4*/+; *UAS-shRNA-Usp8/+* (P{TRiP.HMS01941}attP2)

(G, J) *w*; nos-Gal4, shrb^{G5}*/+; *UAS-shRNA-Usp8/+* (P{TRiP.HMS01941}attP2)

(H) *w*; nos-Gal4*/+; *UAS-shRNA-Usp8/+* (P{TRiP.HMS01941}attP2)

w; nos-Gal4, shrb^{G5}*/+; *UAS-shRNA-Usp8/+* (P{TRiP.HMS01941}attP2)

w; nos-Gal4, shrb^{G5}*/+

Figure 4

(A) *w*; nos-Gal4, shrb^{G5}*/+

w; nos-Gal4, shrb^{G5}/+; UAS-shRNA-Usp8/+* (P{TRiP.HMS01941}attP2)

(B) *w*; nos-Gal4, shrb^{G5}/UAS-Shrb-KR-HA*

(C) *w*; nos-Gal4, shrb^{G5}/+*

w; nos-Gal4, shrb^{G5}/UAS-Shrb-WT-HA*

w; nos-Gal4, shrb^{G5}/UAS-Shrb-KR-HA*

(D) *hs-FLP, nos-Gal4/+; FRT42, Shrb^{G5}/FRT42, Ubi-nls-GFP*

(E) *hs-FLP, nos-Gal4/+; UAS-Shrb-WT-HA ,FRT42, Shrb^{G5} / FRT42, Ubi-nls-GFP*

(F) *hs-FLP, nos-Gal4/+; UAS-Shrb-KR-HA, FRT42, Shrb^{G5} / FRT42, Ubi-nls-GFP*

(G) same as (D, E, F)

Figure 5

(A) *CHMP2B-GFP/+;nos-Gal4/+*

CHMP2B-GFP/+;nos-Gal4/ UAS-shRNA-Usp8/+ (P{TRiP.HMS01941}attP2)

(B) *w*;; Usp8^{KI}/+*

(C) *CHMP2B-GFP/+; bam$^{\Delta 86}$/bam$^{\Delta 86}$, hs-Bam*

(D) *CHMP2B-GFP/+; nos-Gal4/+*

(E) *CHMP2B-GFP/+; bam$^{\Delta 86}$/bam$^{\Delta 86}$, hs-Bam*

Figure S1:

(A) *w*;; nos-Gal4/UAS-shRNA-w* (P{TRiP.GL00094}attP2)

w; UAS-shRNA-Usp8* (P{TRiP.HMS01898}attP40) */+; nos-Gal4*/+

w;; nos-Gal4*/*UAS-shRNA-Usp8* (P{TRiP.HMS01941}attP2)

(B) *w*; UAS-shRNA-Usp8* (P{TRiP.HMS01898}attP40) */+; nos-Gal4*/+

(C) *w*;; nos-Gal4/UAS-shRNA-w* (P{TRiP.GL00094}attP2)

w; UAS-shRNA-Usp8* (P{TRiP.HMS01898}attP40) */+; nos-Gal4*/+

(D) *UAS-tub-PA-GFP/+; nos-Gal4, UAS-par1-GFP/ UAS-shRNA-Usp8* (P{TRiP.GL00094}attP2)

(E) *UAS-tub-PA-GFP/+; nos-Gal4, UAS-par1-GFP/ +*

(F) *nos-Gal4, UAS-par1-GFP/ +*

(G) *nos-Gal4, UAS-par1-GFP/ UAS-shRNA-Usp8* (P{TRiP.GL00094}attP2)

(H) *w*;; nos-Gal4/UAS-shRNA-w* (P{TRiP.GL00094}attP2)

(I) *w*;; nos-Gal4*/*UAS-shRNA-Usp8* (P{TRiP.HMS01941}attP2)

(J-L) *hs-FLP/+;; FRT82, Usp8^{KI}/FRT82, Ubi-nls-RFP*

(M) *w*;; nos-Gal4/UAS-shRNA-w* (P{TRiP.GL00094}attP2)

(N) *w*;; nos-Gal4*/*UAS-shRNA-Usp8* (P{TRiP.HMS01941}attP2)

(O) *w*; tj-Gal4/+*

(P) *w*; tj-Gal4/+*

alix^{1}/alix^{1}

w; tj-Gal4/UAS-Usp8-WT-V5*

w; tj-Gal4/UAS-Usp8-C572A-V5*

Figure S2:

(A) *hs-FLP/+;; FRT82, Usp8^{KI}/FRT82, Ubi-nls-RFP*

(C) *hs-FLP/+;; FRT82, Usp8^{KO}/FRT82, Ubi-nls-RFP*

(D) *hs-FLP/+;bam-Gal4, UAS-Usp8-WT-V5/+; FRT82, Usp8^{KO}/FRT82, Ubi-nls-RFP*

(E) *hs-FLP/+;bam-Gal4, UAS-Usp8-C572A-V5/+; FRT82, Usp8^{KO}/FRT82, Ubi-nls-RFP*

(F) *hs-FLP/+;bam-Gal4, UAS-Usp8-C572A-V5/+; FRT82, Usp8^{KO}/FRT82, Ubi-nls-GFP*

(G) *bam-Gal4, UAS-Usp8-C572A-V5*/ TI{TI}Rab5^{EYFP}

(H) *bam-Gal4, UAS-Usp8-C572A-V5*/+; TI{TI}Rab7^{EYFP}/+

(I,J) *w*;; Usp8^{KI}/+*

Figure S3:

(F) *shrb^{KI}/+*

(G) *shrb^{KI}/+ ; nos-Gal4/ UAS-shRNA-Usp8* (P{TRiP.HMS01941}attP2)

(H,I) *CHMP2B-GFP$^{PBac\{fTRG00825.sfGFP-TVPTBF\}}$/+*

(J) *hs-FLP/+; CHMP2B-GFP$^{PBac\{fTRG00825.sfGFP-TVPTBF\}}$/+; FRT82, Usp8^{KO}/FRT82, Ubi-nls-RFP*

(K, L) *w**

(M) *hs-FLP/+;; FRT82, Usp8^{KO}/FRT82, Ubi-nls-RFP*

(N) *nos-Gal4, UAS-Shrb-WT-HA/+*

(O) *nos-Gal4, UAS-Shrb-WT-HA/+; UAS-shRNA-Usp8/+* (P{TRiP.HMS01941}attP2)

(P) *CHMP2B-GFP$^{PBac\{fTRG00825.sfGFP-TVPTBF\}}$/+;nos-Gal4/+*

(Q) *CHMP2B-GFP$^{PBac\{fTRG00825.sfGFP-TVPTBF\}}$/+;nos-Gal4/UAS-shRNA-Usp8/+* (P{TRiP.HMS01941}attP2)

(R) *w*; nos-Gal4/+; UAS-shRNA-Usp8/+* (P{TRiP.HMS01941}attP2)

w; nos-Gal4, shrb^{G5}/+; UAS-shRNA-Usp8/+* (P{TRiP.HMS01941}attP2)

(S) *UAS-GFP/+; nos-Gal4/UAS-shRNA-Usp8* (P{TRiP.HMS01941}attP2)

*UAS-shRNA-CHMP2B(*P{TRiP.HMS01844}attP40*)/+;nos-Gal4/UAS-shRNA-Usp8* (P{TRiP.HMS01941}attP2)

*UAS-shRNA-CHMP2B(*P{TRiP.HMS01844}attP40*/+;nos-Gal4/UAS-shRNA-w* (P{TRiP.GL00094}attP2)

(T) *UAS-GFP/+; nos-Gal4/UAS-shRNA-Usp8* (P{TRiP.HMS01941}attP2) *UAS-shRNA-CHMP2B(*P{TRiP.HMS01844}attP40*/+;nos-Gal4/UAS-shRNA-w* (P{TRiP.GL00094}attP2)

Figure S4:

(C) *w*; nos-Gal4, shrb^{G5}/UAS-Shrb-WT-HA*

(E) *hs-FLP, nos-Gal4//+; UAS-Shrb-KR-HA, FRT42, Shrb^{G5} / FRT42, Ubi-nls-GFP*